

Substituted Phenyl 4-(2-Oxoimidazolidin-1-yl)benzenesulfonamides as Antimitotics. Antiproliferative, Antiangiogenic and Antitumoral Activity, and Quantitative Structure-Activity Relationships

Sébastien Fortin ^{a,b,*}, Lianhu Wei ^c, Emmanuel Moreau ^d, Jacques Lacroix ^a, Marie-France Côté ^a, Éric Petitclerc ^{a,e}, Lakshmi P. Kotra ^{c,f}, René C.-Gaudreault ^{a,g,*}

^a Unité des Biotechnologies et de Bioingénierie, Centre de recherche, C.H.U.Q., Hôpital Saint-François d'Assise, Québec, Québec, Canada G1L 3L5, e-mail: sebastien.fortin.1@ulaval.ca, jacques.lacroix@crsfa.ulaval.ca, marie-france.cote@crsfa.ulaval.ca, rene.c-gaudreault@crsfa.ulaval.ca

^b Faculté de Pharmacie, Université Laval, Pavillon Vandry, Québec, Québec, Canada G1V 0A6

^c Center for Molecular Design and Preformulations, Toronto General Research Institute, University Health Network, Toronto, Ontario, Canada M5G 1L7, e-mail: william.wei@utoronto.ca, lkotra@uhnresearch.ca

^d Clermont 1, Université d'Auvergne, Inserm, U 990, F-63000 Clermont-Ferrand, France, e-mail: emmanuel.moreau@u-clermont1.fr

^e Present address: Héma-Québec, 1070, avenue des Sciences-de-la-Vie, Québec, Québec, Canada G1V 5C3, e-mail: eric.petitclerc@hema-quebec.qc.ca

^f Department of Pharmaceutical Sciences, Leslie Dan Faculty of Pharmacy, University of Toronto, Toronto, Ontario, Canada M5S 3M2

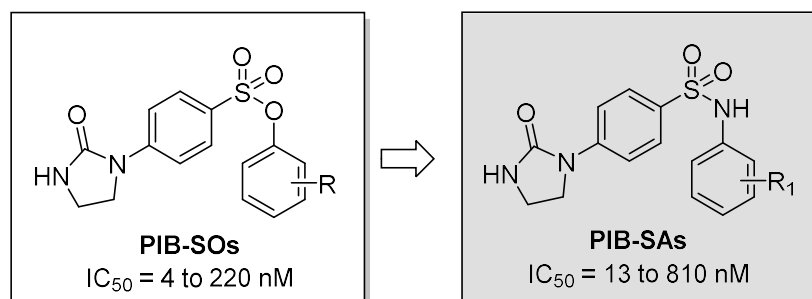
§ Faculté de Médecine, Université Laval, Pavillon Vandry, Québec, Québec, Canada G1V 0A6

***Corresponding authors:** Sébastien Fortin; Phone: 418-525-4444 ext. 52364, Fax: 418-525-4372, e-mail: sebastien.fortin.1@ulaval.ca or René C.-Gaudreault; Phone: 418-525-4444 ext. 52363, Fax: 418-525-4372, e-mail: rene.c-gaudreault@crsfa.ulaval.ca. Unité des Biotechnologies et de Bioingénierie, C.R.C.H.U.Q, Hôpital Saint-François d'Assise, 10, rue de l'Espinau, Québec (Québec) CANADA, G1L 3L5

Abbreviations List: phenyl 4-(2-oxoimidazolidin-1-yl)benzenesulfonate, PIB-SO; phenyl 4-(2-oxoimidazolidin-1-yl)benzenesulfonamide, PIB-SA; colchicine-binding site, C-BS; chick chorioallantoic membrane tumor assays, CAM assays; *N,N'*-ethylene-bis(iodoacetamide), EBI.

Graphical abstract

Forty one phenyl 4-(2-oxoimidazolidin-1-yl)benzenesulfonamide (PIB-SA) derivatives were prepared and biologically evaluated. PIB-SAs are a new class of potent antimicrotubule agents binding to the C-BS.



Highlights

- ❖ PIB-SA is new class of antimitotics exhibiting a new molecular scaffold.
- ❖ PIB-SAs arrest the cell cycle progression in G2/M phase.
- ❖ PIB-SAs are potent antimicrotubule agents binding to the C-BS.
- ❖ PIB-SAs were not or only slightly affected by chemoresistance.
- ❖ PIB-SAs exhibit potent antitumoral and antiangiogenic activity in the CAM assay.

Abstract

The importance of the bridge linking the two phenyl moieties of substituted phenyl 4-(2-oxoimidazolidin-1-yl)benzenesulfonates (PIB-SOs) was assessed using a sulfonamide group, which is a bioisostere of sulfonate and ethenyl groups. Forty one phenyl 4-(2-oxoimidazolidin-1-yl)benzenesulfonamide (PIB-SA) derivatives were prepared and biologically evaluated. PIB-SAs exhibit antiproliferative activities at the nanomolar level against sixteen cancer cell lines, block the cell cycle progression in G₂/M phase, leading to cytoskeleton disruption and anoikis. These results were subjected to CoMFA and CoMSIA analyses to establish quantitative structure-activity relationships. These results evidence that the sulfonate and sulfonamide moieties are reciprocal bioisosteres and that phenylimidazolidin-2-one could mimic the trimethoxyphenyl moiety found in the structure of numerous potent antimicrotubule agents. Finally, compounds **16** and **17** exhibited potent antitumor and antiangiogenic activities on HT-1080 fibrosarcoma cells grafted onto chick chorioallantoic membrane similar to CA-4 without significant toxicity for the chick embryos, making this class of compounds a promising class of anticancer agents.

Keywords. Phenyl 4-(2-oxoimidazolidin-1-yl)benzenesulfonamides; PIB-SA; Antimicrotubule agents; Anticancer drugs; Antimitotic agents.

1. Introduction

Cancer is the second cause of death in North America after cardiovascular diseases. About 569,490 Americans are expected to die of cancer in 2010 [1]. Moreover, according to a new edition of the World Cancer Report 2008, cancer is going to be the leading cause of death worldwide by 2010 [2]. In addition, number of global cancer deaths is projected to increase by 45% from 2007 to 2030, influenced in part by an increasing and aging population [3]. Despite recent breakthroughs, the ability of curing cancer patients remains an elusive goal, with a great need to develop alternative and more effective therapies to improve both life expectancy and quality of life of patients [4].

Microtubules, the key component of the cytoskeleton are composed of α -, β -tubulin heterodimers. Microtubules are also one of the most successful cancer chemotherapeutic targets since they are responsible for mitotic spindle formation and proper chromosomal separation [5]. Antimicrotubule agents such as *vinca* and *taxus* alkaloids play important roles in the treatment of wide variety of cancers [6, 7]. However, poor water solubility, unfavourable biodistribution, significant dose-limiting toxicity, and multidrug resistance mechanisms limit their use and their efficacy [5, 8, 9]. In that context, several academic and industrial groups focus their efforts to develop new antimicrotubule agents to circumvent these limitations. Several antimitotics exhibiting vascular disrupting properties are under evaluation in phase I to phase III clinical trials [10, 11]. Drugs such as combretastatin A-4 sodium phosphate (**1**, CA-4P), a water soluble prodrug of combretastatin A-4 (**2**, CA-4) isolated from *Combretum caffrum*, have received much attention in recent years due to its simple stilbene structure, its high potency as colchicine-binding site (C-BS) antagonist and its potent antitumoral activity [12, 13]. CA-4P represents a promising drug in various clinical settings showing potent activity by reducing significantly the tumoral blood flow [14].

However, CA-4P shows many deleterious effects such as hypertension, hypotension, tachycardia, tumor pain and lymphopenia [10], and is hampered by a short biological half-life [15, 16] and biological instability [17, 18]. Consequently, the search for novel antimicrotubule agents is still required to improve the biopharmaceutical and pharmacological properties of that class of compounds. To that end, we recently reported a new class of antimitotic agents named phenyl 4-(2-oxoimidazolidin-1-yl)benzenesulfonate (**3**, PIB-SO) [19] where the trimethoxyphenyl moiety of CA-4 sulfonate (**4**) is replaced by a phenylimidazolidin-2-one moiety. PIB-SOs are potent antiproliferative agents exhibiting IC₅₀ in the low nanomolar range on several tumor and chemoresistant cell lines. PIB-SOs were also found to bind to the C-BS, arresting the cell cycle in G₂/M phase, leading to the disruption of the cytoskeleton and apoptosis. Of interest, the structure-activity relationship studies of PIB-SOs suggest that the phenylimidazolidin-2-one moiety (ring A of PIB-SOs) may mimic the trimethoxyphenyl moiety CA-4 (ring A of CA-4), which is commonly found in the design of potent antimicrotubule agents and described as a key structural element for the binding of antimitotics to the C-BS [20]. PIB-SOs bearing a 3-chloro, a 3,5-dimethoxy or a 3,4,5-trimethoxy group have also shown potent antitumoral and antiangiogenic potency in the chick chorioallantoic membrane tumor assays (CAM assay). The latter are at least as potent as CA-4 and exhibit low to very low toxicity on the chick embryos evidencing PIB-SOs as promising anticancer drugs.

Sulfonamide group has received a great deal of attention due to its relatively simple structure and the wide variety of drugs such as anti inflammatory [21, 22], diuretics [23], anticonvulsants [24, 25], antiepileptics [26], cox-2 inhibitors [27] and hypoglycemic [28] that are based on its presence. That group is also found in potent new antimicrotubule agents such as 2-fluoro-1-methoxy-4-pentafluorophenylsulfonamidobenzene (**5**, T138067) [29-31], *N*-[2-[(4-hydroxyphenyl)amino]-3-pyridinyl]-4-methoxybenzenesulfonamide (**6**,

ABT-751) [32-36] and *N*-[1-(4-methoxybenzenesulfonyl)-2,3-dihydro-1*H*-indol-7-yl]-isonicotinamide (7, J30) [37, 38] binding to the C-BS. In addition, sulfonamide and sulfonate groups are considered as reciprocal bioisosteres [39]. In this context, we have further investigated the importance of the sulfonate moiety bridge in the structure-activity relationships of PIB-SO by converting the sulfonate moiety of PIB-SO into a sulfonamide moiety leading to the formation of phenyl 4-(2-oxoimidazolidin-1-yl)benzenesulfonamides (**8-48**, PIB-SAs). In this study, we assessed the effect of the nature and the position of the substituents on the aromatic ring B of new PIB-SAs (Fig. 1). We are describing their preparation, antiproliferative activity on several human cancer cell lines and their antitumoral and antiangiogenic potency in human fibrosarcoma HT-1080 grafted onto the chorioallantoic membrane of developing chick embryos (CAM assay). We also prepared CoMFA and CoMSIA models to establish some of the QSAR ruling the biological activity of PIB-SAs.

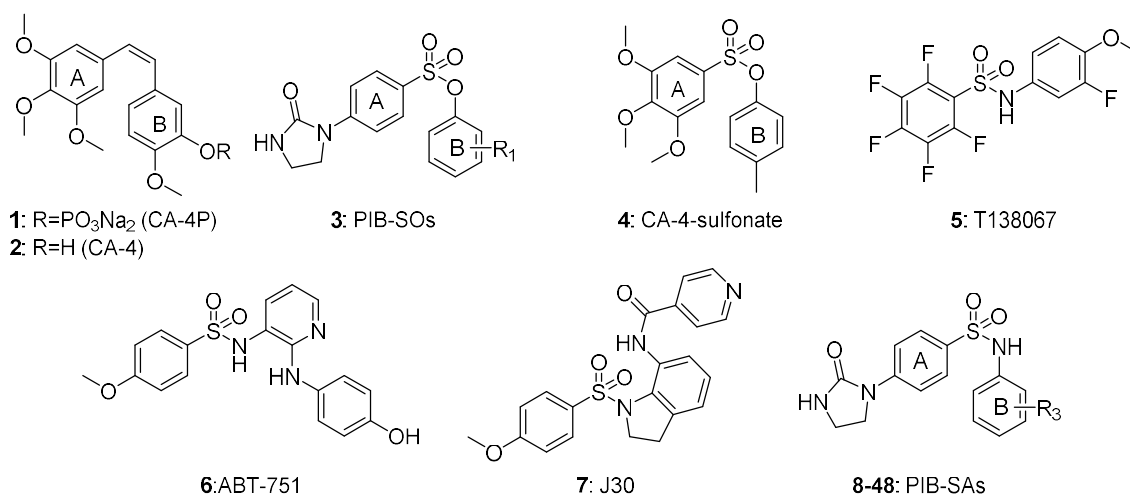
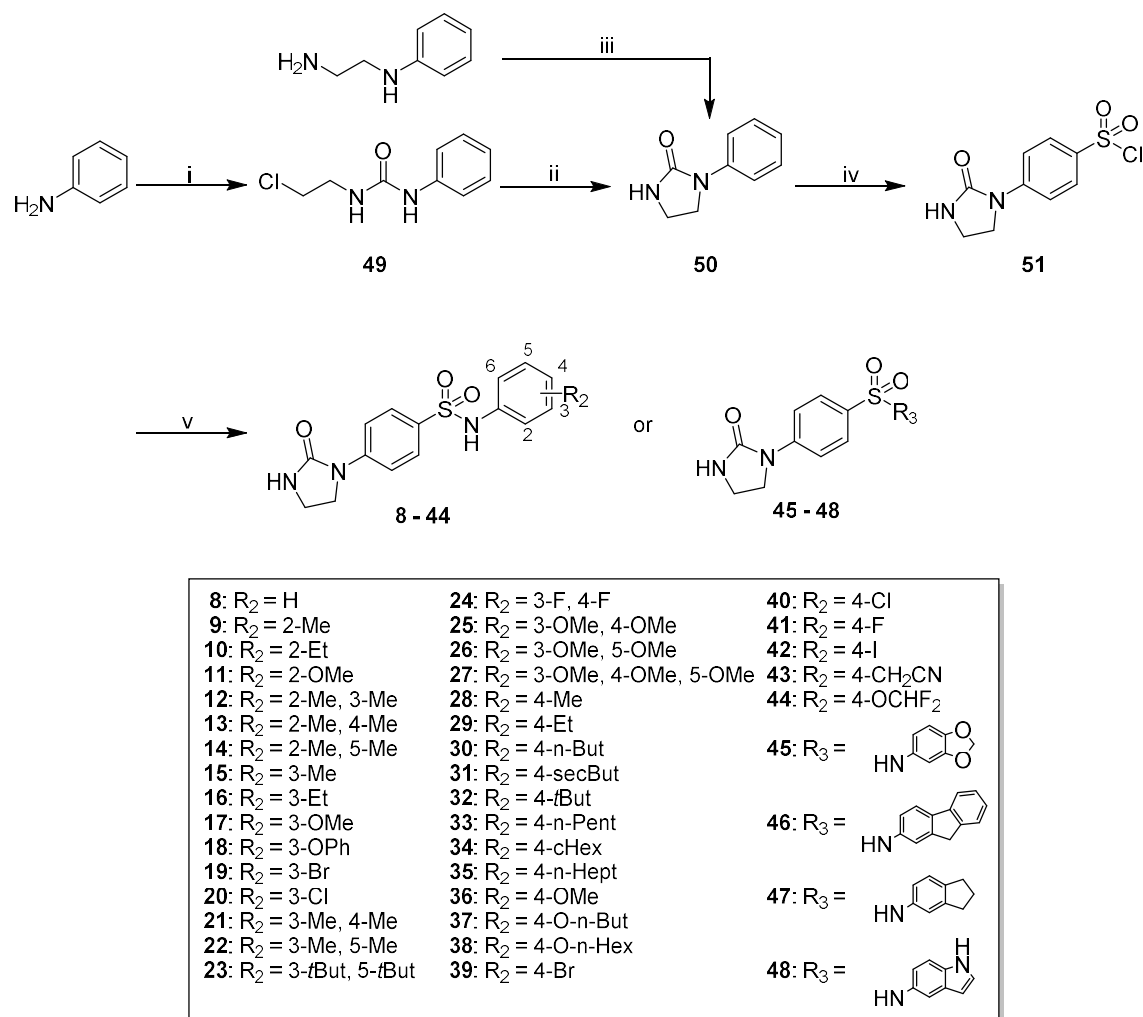


Fig. 1. Molecular structures of CA-4P (1), CA-4 (2), PIB-SOs (3), CA-4-sulfonate (4), T138067 (5), ABT-751 (6), J30 (7) and PIB-SAs (8-48).

2. Chemistry

The method used for the preparation of PIB-SAs (**8-48**) is described in Scheme 1. Compound **51** was prepared as published previously [40, 41]. Briefly, 1-phenylimidazolidin-2-one (**50**) was obtained by the nucleophilic addition of aniline to 2-chloroethylisocyanate in methylene chloride at 25 °C followed by cyclization of the 1-(2-chloroethyl)-3-phenylurea (**49**) using sodium hydride in THF at 25 °C. Compound **50** was also prepared in good yield as previously described by Neville et al [40] using triphosgene with *N*-phenylethylenediamine and triethylamine in tetrahydrofuran at 0 °C. 4-(2-Oxoimidazolidin-1-yl)benzene-1-sulfonyl chloride (**51**) was obtained by chlorosulfonation of compound **50** by chlorosulfonic acid in carbon tetrachloride at 0 °C. Compounds **8-48** were then prepared by nucleophilic addition of an appropriate aniline on compound **51** in the presence of 4-dimethylaminopyridine in acetonitrile at 25 °C.



Scheme 1. Reagents: (i) 2-chloroethylisocyanate, DCM; (ii) NaH, THF; (iii) triphosgene, TEA, THF; (iv) ClSO₃H, CCl₄ and (v) relevant aniline, DMAP/CH₃CN.

3. Results

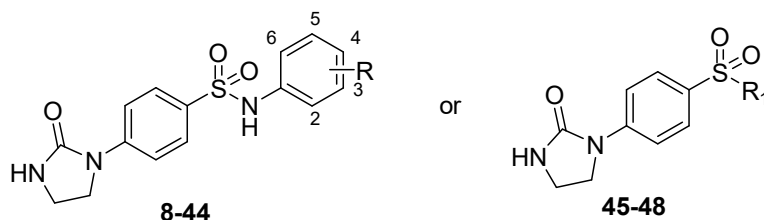
3.1 Antiproliferative Activity

The antiproliferative activity of PIB-SAs **8-48** was assessed initially on three human cancer cell lines, namely, HT-29 colon carcinoma, M21 skin melanoma and MCF-7 breast carcinoma cells. HT-29, M21, and MCF-7 cell lines were selected, as they are good representatives of tumors originating from the three embryonic germ layers. Cell growth inhibition was assessed

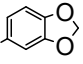
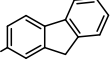
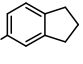
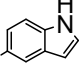
according to the NCI/NIH Developmental Therapeutics Program [42]. The results are summarized in Table 1 and expressed as the concentration of drug inhibiting cell growth by 50% (IC₅₀). Afterward, the biological evaluation of the most potent PIB-SAs exhibiting an IC₅₀ lower than 200 nM on the tumor cell panel were further assessed on a panel of 13 tumor cell lines comprising chemoresistant and sensitive cells, on binding to the C-BS and on CAM assay.

Table 1

Evaluation of the Antiproliferative Activity of PIB-SAs (**8-48**) and CA-4 on HT-29, M21, and MCF-7 Cell Lines.



Compounds	R or R ₁	IC ₅₀ (nM) ^a		
		HT-29	M21	MCF-7
8	R = H	280	200	470
9	R = 2-Me	200	150	280
10	R = 2-Et	240	180	350
11	R = 2-OMe	550	300	770
12	R = 2-Me, 3-Me	190	110	230
13	R = 2-Me, 4-Me	180	150	230
14	R = 2-Me, 5-Me	46	27	48
15	R = 3-Me	110	69	190
16	R = 3-Et	110	82	130
17	R = 3-OMe	120	65	120
18	R = 3-OPh	200	83	220
19	R = 3-Br	77	59	100
20	R = 3-Cl	55	25	79
21	R = 3-Me, 4-Me	230	94	230
22	R = 3-Me, 5-Me	82	63	100
23	R = 3- <i>t</i> But, 5- <i>t</i> But	> 1000	> 1000	> 1000
24	R = 3-F, 4-F	350	220	620
25	R = 3-OMe, 4-OMe	520	340	610
26	R = 3-OMe, 5-OMe	78	60	170
27	R = 3-OMe, 4-OMe, 5-OMe	21	13	18

28	R = 4-Me	480	260	610
29	R = 4-Et	660	480	810
30	R = 4-But	610	450	770
31	R = 4-secBut	> 1000	> 1000	> 1000
32	R = 4- <i>t</i> But	> 1000	> 1000	> 1000
33	R = 4-Pent	990	870	> 1000
34	R = 4-cHex	> 1000	> 1000	> 1000
35	R = 4-Hept	> 1000	> 1000	> 1000
36	R = 4-OMe	800	580	> 1000
37	R = 4-OBu	630	580	870
38	R = 4-OHex	> 1000	> 1000	> 1000
39	R = 4-Br	300	130	240
40	R = 4-Cl	220	90	170
41	R = 4-F	370	230	690
42	R = 4-I	650	260	600
43	R = 4-CH ₂ CN	> 1000	> 1000	> 1000
44	R = 4-OCHF ₂	650	410	760
45	R ₁ = HN 	280	190	460
46	R ₁ = HN 	450	370	480
47	R ₁ = HN 	190	130	240
48	R ₁ = HN 	130	87	170
CA-4		61	4.3	5.6

^aIC₅₀: Expressed as the concentration of drug inhibiting cell growth by 50%.

3.2 Antiproliferative Activity of Most Potent PIB-SAs on Chemoresistant and Sensitive Cancer Cells

The antiproliferative activities of most potent PIB-SA derivatives **14-17**, **19**, **20**, **22**, **26**, **27** and **48** exhibiting an IC₅₀ under 200 nM on HT-29, M21 and MCF-7 tumor cell lines were assessed on ten sensitive and three chemoresistant cell lines. Sensitive cells were Chinese hamster ovary CHO, human chronic myelogenous leukemia K562, murine lymphocytotic leukemia L1210, murine macrophages P388D1, murine melanoma B16F0, human prostate carcinoma DU 145, human fibrosarcoma HT-1080, human breast adenocarcinoma MDA-MB-

231, human ovarian SKOV3 and T cell leukemia CEM cells, respectively. Resistant cancer cell lines were paclitaxel-resistant CHO-TAX 5-6 [43], colchicine- and vinblastine-resistant CHO-VV 3-2 [44] and multidrug-resistant leukemia CEM-VLB [45, 46] cells. The results are summarized in Tables 2 and 3. Colchicine, paclitaxel and vinblastine were used as positive control. IC₅₀ expressed the concentration of drug inhibiting cell growth by 50% and was assessed according to the NCI/NIH Developmental Therapeutics Program [42].

Table 2

Evaluation of the Antiproliferative Activity of Compounds **14-17**, **19**, **20**, **22**, **26**, **27**, **48**, Colchicine, Paclitaxel and Vinblastine on Selected Cancer Cells.

Compd	IC ₅₀ (nM) ^d									
	CHO	K562	L1210	P388D1	B16F0	DU 145	HT-1080	MDA-MB-231	SKOV3	CEM
14	77	72	81	79	86	1610	65	110	72	74
15	230	200	180	250	290	580	210	1270	200	200
16	230	230	200	250	270	730	200	1410	230	200
17	330	230	240	250	370	650	200	730	240	260
19	250	87	99	90	270	340	170	290	170	110
20	96	69	77	78	190	230	68	200	70	77
22	210	110	110	210	260	430	150	1220	190	170
26	330	110	110	200	280	700	150	340	170	170
27	190	19	21	38	58	51	17	45	22	23
48	1310	340	260	520	770	1370	230	3600	280	410
Col^a	220	6.8	6.9	28	13	10	1.1	2.9	2.1	7.9
Pac^b	170	0.71	0.40	35	28	1.3	0.15	9.1	2.6	0.27
Vbl^c	17	0.36	0.16	1.8	0.099	0.063	0.099	0.12	0.039	0.38

^aCol, colchicine; ^bPac, paclitaxel; ^cVbl, vinblastine; ^dIC₅₀: Expressed as the concentration of drug inhibiting cell growth by 50%.

Table 3

Evaluation of the Antiproliferative Activity of Compounds **14-17**, **19**, **20**, **22**, **26**, **27**, **48**, Colchicine, Paclitaxel and Vinblastine in Selected Chemoresistant Cancer Cell Lines.

Compd	IC ₅₀ (nM) ^d	Ratio chemoresistant/ sensitive ^e			Ratio chemoresistant/ sensitive ^e		
		CHO-TAX 5-6 ^f	CHO-TAX 6/CHO	5-CHO-VV 3-2 ^g	CHO-VV 2/CHO	3-CEM-VLB ^h	CEM-VLB/CEM
14	54	0.70	110	1.4	120	1.6	
15	150	0.65	280	1.2	370	1.9	
16	140	0.61	250	1.1	450	2.3	
17	200	0.61	450	1.4	700	2.7	
19	76	0.30	270	1.1	250	2.3	
20	58	0.60	150	1.6	170	2.2	
22	120	0.57	250	1.2	400	2.4	
26	220	0.67	690	2.1	1010	5.9	
27	170	0.89	> 250	>1.3	> 250	> 11	
48	640	0.49	1860	1.4	4840	12	
Col^a	140	0.64	620	2.8	360	46	
Pac^b	520	3.1	140	0.82	3340	12370	
Vbl^c	6.9	0.41	66	3.9	600	1579	

^aCol, colchicine; ^bTax, paclitaxel; ^cVbl, vinblastine; ^dIC₅₀: Expressed as the concentration of drug inhibiting cell growth by 50%; ^eRatio is the IC₅₀ of the resistant cells divided by the IC₅₀ of their deriving not resistant cells (CHO and CEM cells); ^fPaclitaxel-resistant CHO-TAX 5-6 cell line; ^gColchicine-and vinblastine-resistant CHO-VV 3-2 cell line; ^hmultidrug-resistant leukemia CEM-VLB cell line.

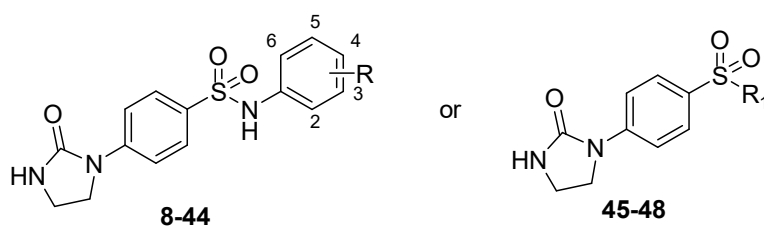
3.3 Binding of PIB-SAs to the Colchicine-Binding Site

The bioisosteric PIB-SOs are C-BS antagonists disrupting the polymerization of tubulin heterodimer, inhibiting cell division in G₂/M phase and leading to anoikis. Therefore, we have conducted experiments to assess the binding of the most potent PIB-SAs to the C-BS on β -tubulin. We first assessed their effects on the cell cycle progression. Table 4 shows the percentage of M21 cells in G₀/G₁, S, and G₂/M phases, respectively, after treatment with most potent PIB-SAs and CA-4 at 5-times their respective IC₅₀ and DMSO used as excipient. Thereafter, we used a simple detection technique developed by our research group to assess the binding of antimicrotubule agents to the C-BS when in competition with *N,N'*-ethylene-bis(iodoacetamide) [47] (EBI). Table 4 shows the results obtained from the competition


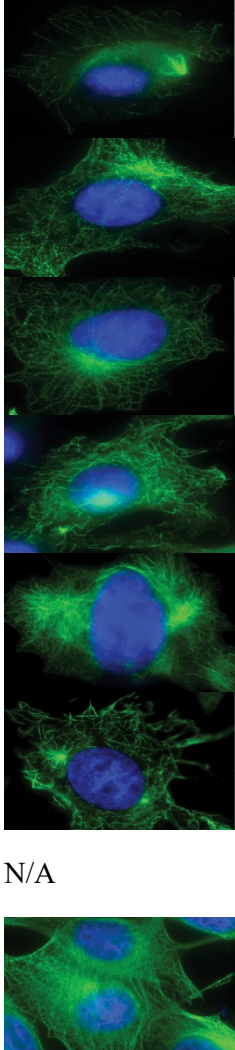


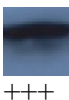
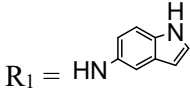
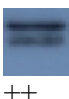

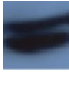
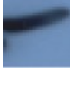
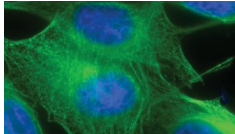
between EBI at 100 μ M and PIB-SAs at 1000-times their IC₅₀ on M21 cells [47]. Finally, the effects of PIB-SAs on the cytoskeleton were also assessed using a fluorescent anti- β -tubulin antibody and immunofluorescence techniques (Table 4).

Table 4

Effect of Selected PIB-SAs **14-17**, **19**, **20**, **22**, **26**, **27**, **48** and CA-4 on Cell Cycle Progression, in the Competition Assay with EBI and on the Cytoskeleton Integrity.



Compd	R, R ₁	Cell cycle progression ^a			Competition with EBI ^{b, c}	Cytoskeleton integrity
		G ₀ /G ₁ (%)	S (%)	G ₂ /M (%)		
14	R = 2-Me, 5-Me	1	20	79	 ++	
15	R = 3-Me	1	16	83	 +++	
16	R = 3-Et	0	5	95	 +++	
17	R = 3-OMe	10	29	61	 +++	
19	R = 3-Br	2	20	78	 +++	

20	R = 3-Cl	5	33	62		
22	R = 3-Me, 5-Me	1	21	78		
26	R = 3-OMe, 5-OMe	13	28	59		
27	R = 3-OMe, 4-OMe, 5-OMe	12	12	74		
48		27	22	51		
CA-4		2	0	98		
EBI		N/A	N/A	N/A		
DMSO		61	30	9		

^aFor cell cycle progression, M21 cells were incubated for 24 h, in presence of PIB-SAs at 5-times their respective IC₅₀; ^bFor the competition assay using EBI, MDA-MB-231 cells were incubated for 2h in presence of PIB-SAs at 1000-times their IC₅₀ then for 1.5 h in presence of EBI; ^cInhibition of EBI coding: +++: Strong inhibition; ++: mild inhibition; +: weak inhibition; -: no inhibition; N/A: not applicable; ^d M21 cells were incubated for 16 h with the drugs at 5-times their IC₅₀ and the cytoskeleton was visualized using indirect immunofluorescence techniques.

3.4 Comparative Molecular Similarity Indices and Comparative Molecular Field Analyses (CoMSIA and CoMFA) of PIB-SAs

CoMSIA and CoMFA were conducted to understand the mechanism underlying the binding of PIB-SAs to the C-BS and to design new and more selective C-BS antagonists. We used Surfex-Sim which is a 3D molecular similarity optimization and searching program that uses a morphological similarity function and fast pose generation based similarity on a molecule's

shape, hydrogen bonding, and electrostatic properties techniques to generate alignments of molecules [48]. The multiple alignments of the most active compounds gave the best description of the positions of functional groups leading to the hypothesis generation. Underlying assumption in the alignment is that the compound with better fit to the hypothesis on structural alignment would have better activity. At first, a mutual alignment on the most active compounds was performed and tried to find a superposition of all input molecules that maximizes the similarity and minimizes the overall volume of the superposition. A hypothesis was generated from this superposition, and that hypothesis will be used as a template to align the set of active molecules. Then the alignment of the dataset will be used to generate QSAR models. Compounds **15**, **20**, **22**, **27**, **40**, and **48** were chosen to generate hypothesis using SYBYL Surfex-Sim mutual alignment module. The alignment hypothesis shows that the groups of same property are well aligned (Fig. 2A). Then all PIB-SAs were superimposed on to the alignment hypothesis using Surfex-Sim flexible superposition module (Fig. 2B). Observing from the q^2 and r^2_{cv} values, the analysis that includes the similarity data to the hypothesis improved the r^2_{cv} value in both CoMFA and CoMSIA models (models A, B, C vs. models D, E, F, models G, H, I vs. models J, K, L). The antiproliferative activities obtained on HT-29, M21, and MCF-7 cell lines were used as dependent variables to build CoMSIA and CoMFA models. The optimized parameters and the statistical data in the PLS analysis of six CoMSIA models and six CoMFA models are presented in supporting information.

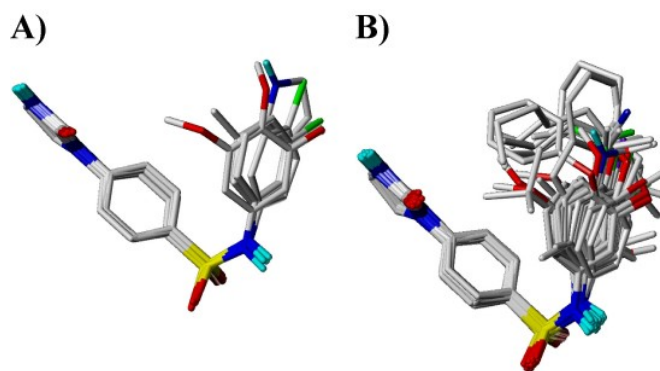


Fig. 2. (A) Alignment hypothesis generated using Surfex-Sim mutual alignment module from compounds **15**, **20**, **22**, **27**, **40**, and **48**. (B) Superposition of in the derivatives of PIB-SAs onto the alignment hypothesis.

3.5 Chick Chorioallantoic Membrane Tumor Assays (CAM assays)

Human HT-1080 fibrosarcoma cells were used to assess the antitumoral activity of PIB-SAs **14-17**, **19**, **20**, **22**, **26**, **27** and **48** in the CAM assay (Fig. 3). Cumulative results are shown from two independent experiments with 10-12 eggs per experiment. No related toxicity was observed on chick embryos treated with the excipient. Untreated eggs were used as negative controls and for normalization of the results. The drugs were administered *iv* at 3 μg per egg except for CA-4 that was used as positive control and was administered *iv* at 1 μg and 3 μg per egg, respectively.

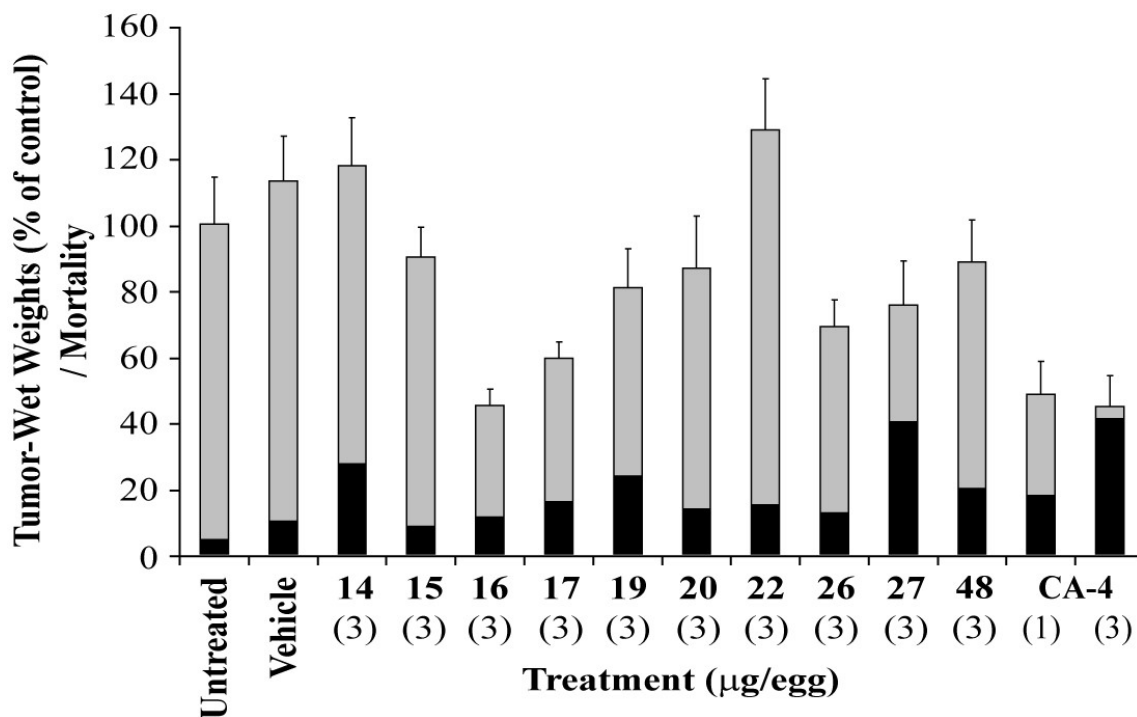


Fig. 3. Growth inhibition of human HT-1080 fibrosarcoma tumors by selected PIB-SAs using the chick chorioallantoic membrane tumor assay (CAM assay). The white histograms represent the percentage of tumor-wet weight of tumor treated by PIB-SAs, CA-4 and the excipient. The black histogram is the percentage of chick mortality.

4. Discussion

4.1 PIB-SAs Inhibit the Proliferation of Human Tumor Cell lines

All compounds, except for compounds **23**, **31-36**, **38** and **43** exhibited antiproliferative activities in the nanomolar range. We classified PIB-SA derivatives into three subgroups based on IC_{50} : (1) high IC_{50} ranging from 13 to 200 nM (**14-17**, **19**, **20**, **22**, **26**, **27** and **48**), (2) fair IC_{50} ranging from 83 to 810 nM (**8-13**, **18**, **21**, **24**, **25**, **28-30**, **39-42** and **44-47**), (3) weak IC_{50} ranging from 580 to > 1000 nM (**23**, **31-38** and **43**) on three tumor cell lines. Among PIB-SA subgroups having high activity, compounds **14**, **20** and **27** bearing a 2,5-dimethyl, a 3-chloro and a 3,4,5-trimethoxy group on ring B, respectively, exhibited antiproliferative

activity equipotent to CA-4 on HT-29 cells. Moreover, compounds having a high IC₅₀ were further evaluated on a panel of 13 chemoresistant and sensitive tumor cell lines, for binding to the C-BS and in the CAM assay. The PIB-SAs **14-17**, **19**, **20**, **22**, **26**, **27** and **48** showed antiproliferative activities on sensitive cancer cells (CHO, K562, L1210, P388D1, B16F0, DU 145, HT-1080, MDA-MB-231, SKOV3, CEM) in the same range as in the three screening human tumor cell lines (Table 2). However, the antiproliferative activity of the most potent PIB-SA was lower than colchicine, paclitaxel or vinblastine.

4.2 Cytotoxicity of PIB-SAs was Unaffected in Drug-Resistant Cells

Table 3 shows the antiproliferative activities of PIB-SAs **14-17**, **19**, **20**, **22**, **26**, **27** and **48** on drug-resistant cell lines CHO-TAX 5-6, CHO-VV 3-2 and CEM-VLB. On one hand, CHO-TAX 5-6 cells are resistant to microtubule stabilizers (e.g., paclitaxel) and hypersensitive to microtubule disruptors (e.g., colchicine, vinblastine) while CHO-VV 3-2 cell line are resistant to microtubule disruptors and hypersensitive to microtubule stabilizers [44]. On the other hand, CEM-VLB cells overexpress P-glycoprotein [49] which is responsible for the cellular efflux of drugs and chemoresistance to anticancer drugs such as doxorubicin, etoposide, paclitaxel and vinblastine [50]. As expected and confirmed in Table 3, CHO-TAX 5-6 cells were resistant to paclitaxel (3.1-fold) and were sensitive to compounds **14-17**, **19**, **20**, **22**, **26**, **27** and **48**, colchicine and vinblastine. Moreover, CHO-VV 3-2 cells were resistant to the colchicine and vinblastine, 2.8- and 3.9-fold respectively and were sensitive to paclitaxel. Unexpectedly and except for compound **26**, CHO-VV 3-2 cells were slightly or not resistant to the PIB-SAs tested. CHO-VV 3-2 cells were resistant to compound **26** (2.1-fold), which was even slightly lower than for colchicine and vinblastine (2.8 and 3.9-fold, respectively). In addition, CEM-VLB cells were resistant to colchicine, vinblastine and paclitaxel, 46-, 12370- and 1579-fold respectively. The antiproliferative activity all PIB-SAs, at the exception of compound **26**, **27** and **48**, was unaffected by the overexpression of P-glycoprotein. CEM-VLB

cells were mildly resistant to compound **26**, **27** and **48**, 5.9-, >11- and 12-fold, respectively, which is more than 4-times lower than for colchicine and several logs lower than for paclitaxel and vinblastine.

4.3 PIB-SAs Arrest the Cell Cycle Progression in G₂/M Phase

Table 4 shows percentage of M21 cells arrested in G₀/G₁, S, and G₂/M phases, respectively, after treatment with PIB-SAs for 24 h at 5-times their respective IC₅₀. Control cells treated with 0.5% DMSO were found to be in G₀/G₁, S, and G₂/M phases at 61%, 30%, and 9%, respectively. Compounds **14**, **15**, **17**, **19**, **20**, **22**, **26**, **27** and **48** strongly blocked cell cycle progression in G₂/M phase; the number of cells in G₂/M phase was increased by 42 to 74%. Compound **16** totally blocked the cell cycle in G₂/M phase; the number of cells in G₂/M phase was increased by 86% as observed with CA-4.

4.4 PIB-SAs Inhibit EBI Binding to the C-BS

As aforementioned, C-BS antagonists such as colchicine, podophyllotoxin, 2-methoxyestradiol and CA-4 inhibit the EBI binding to β -tubulin leading to disappearance of the β -tubulin-EBI adduct formed and detectable by Western blot as a second immunoreacting band of β -tubulin migrating faster than the native β -tubulin [47]. Except for compound **14** and **48** that mildly inhibited the formation of the β -tubulin-EBI adduct, PIB-SAs **15-17**, **19**, **20**, **22**, **26** and **27** strongly abrogated the binding of EBI to the C-BS in a similar fashion as observed with CA-4.

4.5 PIB-SAs Disrupt the Cytoskeleton of Tumor Cells

Table 4 shows the cytoskeleton of M21 cells treated with PIB-SAs at 5-times their respective IC₅₀ for 16 hours. Control M21 cells treated with DMSO are exhibiting homogenous, linear

and structured cytoskeletons while all PIB-SAs tested clearly exhibit disrupted microtubular structures.

4.6 CoMSIA Models

In all CoMSIA models, the contour maps of each type field have very similar coverage areas for different biological activities. Here we took the QSAR CoMSIA contour map of M21 as an example. The optimized CoMSIA model included descriptors of 3D molecular similarity (Surflex-Sim searching program to generate alignments of molecules), polar volume, and molecular energy. The predicted PIB-SA molecular activity values of model A, B, and C are presented in supporting information. CoMSIA model predicted activities of models D, E, and F and contour maps of CoMSIA fields contributing to ligand binding generated by PLS analysis without using similarity descriptor in M21 cell line (Model E) are presented in supporting information. The models showed that compounds with higher similarity to the hypothesis generated from the active compounds tend to have higher activities. In Fig. 4, compound **20** was used as a reference to show the contour map of the CoMSIA model. Fig. 4A shows the favoured (green) and disfavoured (yellow) area of steric field. Most area surrounding the molecule was in favour of steric field. Thus bulky groups have positive contributions to the biological activity when present in ortho and meta positions (compounds **9**, **10**, **12-16**, **21** and **22**). Bulky groups in the 4-position were unfavourable for the activity. That explains most of the compounds bearing bulky group on position 4 such as compounds **28-30**, **31-38**, **42**, and **43** exhibit lower activities. Compounds substituted on position 5 exhibit significantly higher antiproliferative activities (**14**, **22**, **26** and **27**). The effects of electrostatic field are shown in Fig. 4B. Favoured electrostatic field are in blue and disfavoured electrostatic field are in red. The region around the *para*-position accommodates electronegative substituents leading to favourable biological activities (**39** and **40**). Compounds **24**, **25**, **37**, **38** bear highly electronegative atoms such as oxygen and fluorine that

are contributing to weaker activities than that of compound **8**. Fig. 4C illustrates the contribution of hydrophobicity to the antiproliferative activity. Yellow color shows favoured hydrophobic region and cyan color shows disfavoured hydrophobic region. To that end, the most favourable hydrophobic region is around position 3 and 4, although the hydrophobic character is unfavourable in the region on top of the aromatic cloud of the phenyl moiety. This explains in part the potent cytotoxic activities of compounds **12**, **13**, **15**, **16**, **19**, **20**. From Fig. 4D and 4E, there are two regions that are preferred hydrogen bond acceptors: one is the ketyl moiety of the imidazolidone and the other is the sulfonamide group bridging the phenyl rings. The hydrogen bond donor preferred region is adjacent to nitrogen atom of the sulfonamide bridge.

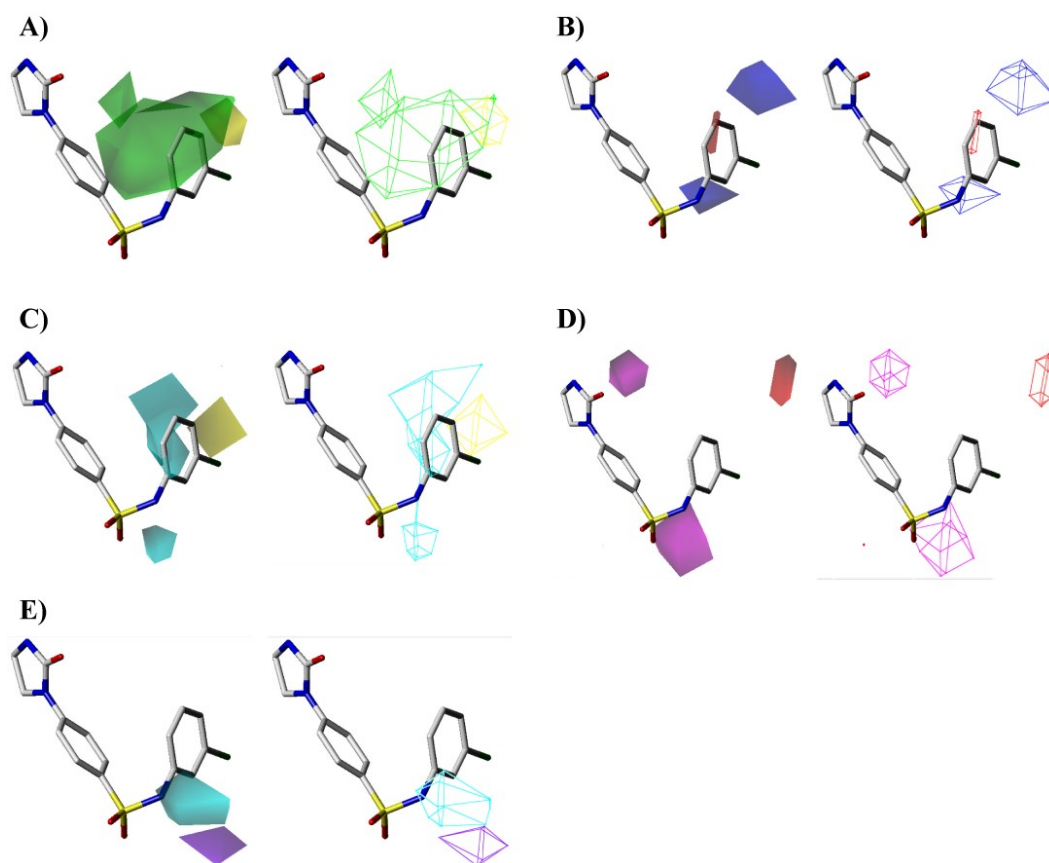


Fig. 4. Contour maps of CoMSIA fields contributing to ligand binding generated by PLS analysis in Model B (M21). Compound **20** (stick model) is shown as a reference to depict the field regions. (A) Contour map of steric field. Green colored map presents favoured steric groups, and yellow colored map presents disfavoured steric groups. (B) Contour map of Electrostatic field. Blue color maps favoured electrostatic field (larger electropositive charge will increase the activity) and red color maps disfavoured electrostatic field (smaller electropositive charge will increase the activity). (C) Contour map of hydrophobic field. Yellow color map shows favoured hydrophobic region and cyan color map shows disfavoured hydrophobic region. (D) Contour map of hydrogen bond acceptor field. Magenta map shows the favoured hydrogen bond acceptor region and red map illustrates hydrogen bond disfavoured region. (E) Contour map of hydrogen bond donor field. Cyan region is hydrogen bond donor preferred region and purple region is the region which hydrogen bond donor is not favoured.

4.7 CoMFA Models

In CoMFA models, M21 activity was used to exemplify our results (Fig. 5). The same descriptors we used in CoMSIA model were also used in this model. The predicted antiproliferative activities for the PIB-SA derivatives based on models G, H, and I are presented in supporting information. CoMFA model predicted activities of models J, K, and L and CoMFA fields contributing to ligand binding generated by PLS analysis without using similarity descriptor in M21 cells (Model K) are presented in supporting information. In CoMFA model, except a small area around position 4 and 5 (yellow region in Fig. 5A), hydrophobic moieties are acceptable at ortho, meta and para positions of phenyl (green maps in Fig. 5A). In terms of electrostatic features, electropositive groups are preferred on position 3 of the phenyl ring (blue map in Fig. 5B) and electronegative groups are preferred on position 5 of the phenyl ring (red maps in Fig. 5B).

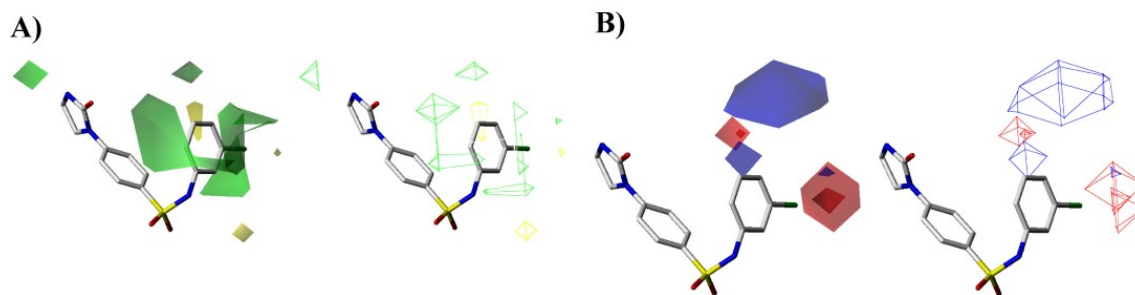


Fig. 5. Contour maps of CoMFA fields contributing to ligand binding generated by PLS analysis in model H (M21). Compound **20** (stick model) was shown in the figure as a reference to depict the field region. (A) Contour map of Steric field. Green map presents the favoured steric interaction from the ligands and the yellow map shows the region that disfavoured steric contribution. (B) Contour map of Electrostatic field. Blue color map depicts favoured electrostatic region, increasing positive charge will contribute to higher activity. Red color map shows the disfavoured electrostatic area, that higher ligand binding do not like higher positive charge.

4.8 PIB-SAs Inhibit the Growth of Solid Tumors in the CAM Assay Model

The growth of solid tumors on the surface of the chick chorioallantoic membrane depends on the ability of the grafted tumor cells to stimulate angiogenesis and to grow significantly within a 7-day period. HT-1080 human fibrosarcoma cells were used because they produce solid tumors that are sensitive to antiangiogenic and antitumoral drugs [51-55]. As shown in Fig. 3, chick embryos have well tolerated the excipient (ethanol: cremophor: phosphate buffer saline: 6.25: 6.25: 87.5) when compared to control embryos (10% and 4% mortality, respectively). All drugs were tested at 3 μg of drug per egg with the exception of CA-4 that was used as a positive control and tested at 1 μg per egg (18% mortality); 3 μg of CA-4 per egg exhibiting high toxicity/mortality rate on chick embryos (45% mortality). CA-4 exhibited a strong vascular disruption and inhibition of tumor growth by 48 and 45%, respectively.

Compounds **14**, **15**, **20**, **22** and **48** had no significant inhibitory effect on the growth of tumor. Except for compound **14** which showed 27% mortality of embryos, compounds **15**, **20**, **22** and **48** showed low toxicity (8 to 18% mortality of embryos). Compounds **19**, **26** and **27** weakly inhibited the growth of tumor (81, 69 and 75% of the control). However, except for compound **26**, which exhibited low toxicity (13% mortality), compounds **19** and **27** showed toxicity (24 and 40% mortality, respectively). Compound **17** inhibited significantly the growth of tumor (59% of the control) and showed low toxicity with 16% mortality of embryos. Finally, compound **16** exhibited good inhibition of the tumor growth similar to CA-4 (45% of the control) with no related toxicity (11% mortality).

5. Conclusions

We identified and described a novel class of antimicrotubule agents acting through its binding to C-BS on tubulin designated as phenyl 4-(2-oxoimidazolidin-1-yl)benzenesulfonamides (PIB-SAs). The aim of this study was to investigate the effect of replacing the sulfonate bridge moiety of PIB-SOs by the sulfonamide reciprocal bioisosteres leading to the formation of PIB-SAs **8-48**. PIB-SAs were synthesized in fair to good yields. They exhibited antiproliferative activities on sixteen cancer cell lines in the nanomolar range and arrested the cell cycle progression in G₂/M phase. Competition assays using EBI and immunofluorescence using anti- β -tubulin antibody confirmed that PIB-SAs are potent antimicrotubule agents binding to the C-BS. In addition, the cytotoxicity of PIB-SAs was not or only slightly affected in chemoresistant cells resistant to colchicine, paclitaxel and vinblastine and in cells bearing the P-glycoprotein. Moreover, quantitative structure-activity relationships of PIB-SA derivatives using CoMSIA and CoMFA were established. These studies provide the evidence that sulfonate and sulfonamide moiety are bioisosteres and phenylimidazolidin-2-one moieties could mimic the trimethoxyphenyl moiety found in the structure of numerous potent

antimicrotubule agents. Finally, PIB-SAs **16** and **17** exhibited potent antitumoral and antiangiogenic potency in the CAM assay, with lower toxicity than CA-4 on chick embryos, making this class of drugs as promising anticancer agents.

6. Experimental protocols

6.1 Biological Methods

6.1.1 Cell Lines Culture

HT-29 human colon carcinoma, MCF7 human breast carcinoma, MDA-MB-231 human breast carcinoma, HT-1080 human fibrosarcoma, K562 human chronic myelogenous leukemia, L1210 murine lymphocytotic leukemia, P388D1 murine macrophages, B16F0 murine skin melanoma, DU 145 human prostate carcinoma and SKOV3 human ovarian were purchased from the American Type Culture Collection (Manassas, VA). Chinese hamster ovary cells (CHO), colchicine- and vinblastine-resistant CHO-VV 3-2 cells and paclitaxel-resistant CHO-TAX 5-6 cells were generously provided by Dr. Fernando Cabral (University of Texas Medical School, Houston, TX) [43, 44]. T cell leukemia CEM cells and multidrug-resistant leukemia CEM-VLB were generously provided by Dr. William T Beck (University of Illinois at Chicago, College of Pharmacy, USA) [45]. M21 human skin melanoma cells were provided by Dr. David Cheresch (University of California, San Diego School of Medicine, USA). B16F0, DU 145, HT-29, HT-1080, M21, MCF7, MDA-MB-231 and SKOV3 cells were cultured in DMEM medium containing sodium bicarbonate, high glucose concentration, glutamine and sodium pyruvate (Hyclone, Logan, UT) supplemented with 5% of calf serum. CHO, CHO-VV 3-2, CHO-TAX 5-6, CEM, CEM-VLB, K562, L1210 and P388D1 cells were cultured in RPMI medium (Hyclone, Logan, UT) supplemented with 10%

of calf serum. The cells were maintained at 37 °C in a moisture-saturated atmosphere containing 5% CO₂.

6.1.2 Antiproliferative Activity Assay

The antiproliferative activity of PIB-SAs (**8-48**) was assessed using the procedure described by the National Cancer Institute for its drug screening program with minor modifications [42]. 96-well microtiter plates were seeded with 75 µL of tumor cell (for HT-29, 5000 cells; M21, 3500 cells; MCF7, 7500 cells; CHO, 1000 cells; K562, 5000 cells; L1210, 6000 cells; P388D1, 18000 cells; B16F0, 2000 cells; DU 145, 5000 cells; HT-1080, 3000 cells; MDA-MB-231, 3000 cells; SKOV3, 5000 cells; CEM, 20000 cells; CHO-VV 3-2, 1000 cells; CHO-TAX 5-6, 1000 cells; CEM-VLB, 20000 cells) in appropriate medium. Plates were incubated at 37 °C, 5% CO₂ for 24 h. Freshly solubilized drugs in DMSO were diluted in fresh medium and aliquots of 75 µL aliquots containing escalating concentrations (1000 to 0.98 nM) of the drug were added. Plates were incubated for 48 h. Plates containing attached cell lines were then stained with sulforhodamine B. Briefly, cells were fixed by addition of cold trichloroacetic acid to the wells (10% (w/v) final concentration), for 30 min at 4 °C. Plates were washed five-times with tap water and dried. Sulforhodamine B solution (50 µL) at 0.1% (w/v) in 1% acetic acid was added to each well, and plates were incubated for 15 min at room temperature. Unbound dye was removed by washing five-times with 1% acetic acid. Bonded dye was solubilized in 10 mM Tris base, and the absorbance was read with a µQuant Universal Microplate Spectrophotometer (Biotek, Winooski, VT) at wavelength between 530 and 565 nm according the color intensity. For cells in suspension resazurin staining was used. Briefly, supernatant was aspirated and 100 µl of resazurin at 25 µg/ml in fresh medium were added. Plates were incubated at 37 °C for 1 to 3 hours according to cell line sensitivity. Fluorescence was read on a FL-500 Fluorometer (Biotek, Winooski, VT) using 530 nm for

excitation wavelength and 590 nm for emission wavelength. The experiments were performed at least in triplicate. The IC₅₀ assay was considered valid when the relative standard deviation was less than 10%.

6.1.3 Cell Cycle Analysis

After incubation of 2.5×10^5 M21 cells with the drugs at 2- and 5-times their respective IC₅₀, for 24 h, the cells were trypsinized, washed with Phosphate Buffered Saline (PBS), resuspended in 250 μ L of PBS, and fixed by the addition of 750 μ L of ice-cold ethanol and stored at -20 °C until use. Thereafter, the cells were centrifuged for 5 min at 1000 g. Cell pellets were washed with PBS and were resuspended in 450 μ L of PBS containing 200 μ g/mL of RNase. After 5 min, 25 μ L of PBS containing 1 mg/mL of propidium iodide was added. Mixtures were incubated on ice for 1 h and then cell cycle distribution was analyzed using an Epics Elite ESP flow cytometer (Coulter Corporation, Miami, FL).

6.1.4 Inhibition of EBI-Binding to β -Tubulin

6-well plates were seeded with MDA-MB-231 cells at 7×10^5 cells per well and incubated for 24 h. Cells were first incubated in presence of approximately 1000-times the IC₅₀ of the drugs for 2 h and afterward they were treated by the addition of EBI (Toronto Research Chemicals, North York, Ontario, Canada) (100 μ M, final concentration) for 1.5 h at 37 °C without changing the culture medium, which contains the drug tested. Control cells were treated with 0.5% dimethylsulfoxide. Afterward, floating and adherent cells were harvested using a rubber policeman, and centrifuged for 3 min at 8 000 rpm. The pellets were washed with 500 μ L of cold PBS and stored at -80 °C until use. The cells pellets were resuspended in PBS and lysed by sonication. The protein concentration was determined using the Bio-Rad protein assay (Bio-Rad laboratories, Mississauga, Canada) Samples were prepared to obtain protein at a

concentration of 2 mg/ml in Laemmli [56] sample (60 mM Tris-Cl pH 6.8, 2% SDS, 10% glycerol, 5% β -mercaptoethanol, 0.01% bromophenol blue). Cell extracts were boiled for 5 min. Twenty micrograms of proteins from the protein extracts were subjected to electrophoresis using 10% polyacrylamide gels. The proteins were transferred onto nitrocellulose membranes that were incubated with TBSMT (Tris-Buffered Saline + 0.1% (v/v) Tween-20 with 2.5% fat-free dry milk) for 1 h at room temperature, and then with the anti- β -tubulin (clone TUB 2.1) (Sigma-Aldrich, St. Louis, MO) primary antibody in TBSMT (1:500) for 16 h at 4 °C. Membranes were washed with TBST (Tris-Buffered Saline with + 0.1% (v/v) Tween-20) and incubated with peroxidase-conjugated anti-mouse immunoglobulin (Amersham Canada, Oakville, Canada) in TBSMT (1:2500) for 2.5 h at room temperature. After washing the membranes with TBST, detection of the immunoblot was carried out with an enhanced chemiluminescence detection reagent kit provided by Amersham Canada (Oakville, Canada).

6.1.5 Fluorescence Microscopy

M21 cells were seeded at 1×10^5 cells per well in 6-well plates that contained 22- μ m glass coverslips coated with fibronectin (10 μ g/mL) and incubated for 24 h at 37 °C. Tumor cells were incubated either with most potent PIB-SAs **14-17**, **19**, **20**, **22**, **26**, **27**, **48** or compound **2** at five-times their respective IC_{50} or DMSO (0.5%) for 16 h. Afterward, the cells were washed twice with PBS, and then fixed with 3.7% formaldehyde in PBS for 20 min. After two washes with PBS, the cells were permeabilized with 0.1% saponin in PBS and blocked with 3% (w/v) BSA in PBS for 1 h at 37 °C. The cells were then incubated for 2 h at 37 °C with the anti- β -tubulin (clone TUB 2.1) in a solution containing 0.1% saponin and 3% BSA in PBS (1:200). The cells were washed five-times with PBS containing 0.05% Tween 20™ and incubated for 1 h at 37 °C in blocking buffer containing anti-mouse IgG Alexa-488

(Molecular Probes, Eugene, OR) (1:1000), 4',6'-diamidino-2-phenylindole (2.5 µg/mL in PBS) to stain the cellular nuclei (1:2000). Cells were then mounted on a microscope slide overnight with slow fade reagent (DakoCytomation, Carpinteria, CA) before analysis using a Olympus BX51 microscope. Images were captured as 8-bit tagged image format files with a Q imaging RETIGA EXI digital camera driven by Image Pro Express software.

6.1.6 CAM Assay

Human HT-1080 fibrosarcoma cells were used to assess the antitumoral activity of PIB-SAs in the CAM assay [52, 53, 57]. Briefly, fertilized chicken eggs purchased from Couvoirs Victoriaville (Victoriaville, Qc, Canada) were incubated for 10 days in a Pro-FI egg incubator fitted with an automatic egg turner before being transferred to a Roll-X static incubator for the rest of the incubation time (both incubators were purchased from Lyon Electric, Chula Vista, San Diego, CA). The eggs were kept at 37 °C in a 60% humidity atmosphere for the whole incubation period. On day-10, using a hobby drill (Dremel, Racine, WI), a hole was drilled on the side of the egg, and a negative pressure was applied to create a new air sac. A window was opened on this new air sac and was covered with transparent adhesive tape to prevent contamination. A freshly prepared cell suspension (40 µL) of HT-1080 (3.5×10^5 cells/egg) cells was applied directly on the freshly exposed chick chorioallantoic membrane tissue through the window. On day-11, the tested drugs dissolved in DMSO were extemporaneously diluted in the excipient (6.25% of ethanol 99%, 6.25% of cremophor and 87.5% phosphate buffer saline). The tested drugs in 100 µL of excipient were injected *iv* in 10–12 eggs. The eggs were incubated until day-17, at which time the embryos were euthanized at 4 °C followed by decapitation. Tumors were collected, and the tumor-wet weights were recorded. The number of dead embryos and signs of toxicity from the different groups were recorded.

6.2 Chemistry

Proton NMR spectra were recorded on a Bruker AM-300 spectrometer (Bruker, Germany). Chemical shifts (δ) are reported in parts per million. IR spectra were recorded on a Magna FT-IR spectrometer (Nicolet instrument corporation, Madison, WI, USA). Uncorrected melting points were determined on an electrothermal melting point apparatus. HPLC analyses were performed on an Acquity UPLC Sample and binary solvent manager equipped with a Quattro Premier™ XE tandem quadrupole mass spectrometer (Waters, Milford, MA, USA). A Waters BECH C18 reversed-phase column (1.7 μ m, 2.1 x 50 mm, 50°C) was eluted in 7 min with a methanol/water linear gradient containing 0.1% TFA at 0.6 mL/min. The purity of compounds was greater than 95%. All reactions were conducted under a dried nitrogen atmosphere. Chemicals were supplied by Aldrich Chemicals (Milwaukee, WI, USA) or VWR International (Mont-Royal, Qc, Canada). Liquid flash chromatography was performed on silica gel F60, 60 A, 40-63 μ m (Silicycle, Québec, Qc, Canada) using a FPX flash purification system (Biotage, Charlottesville, VA, USA) and using the indicated solvent mixture expressed as volume/volume ratios. Solvents and reagents were used without purification unless specified otherwise. The progress of all reactions was monitored using TLC on precoated silica gel plates 60 F254 (VWR international, Mont-Royal, Qc, Canada). The chromatograms were viewed under UV light at 254 and/or 265 nm.

6.3 General Preparation of Compounds 8 to 48.

Compound **51** (1.00 mmol) was suspended in dry acetonitrile (10 mL) under nitrogen atmosphere. Relevant aniline (1.00 mmol) and 4-dimethylaminopyridine (4.00 mmol) were successively added dropwise and the mixture was stirred at room temperature for 48 h. Ethyl acetate was added and the solution was washed with hydrochloric acid 1N, brine, dried over sodium sulfate, filtered, and evaporated to dryness under vacuum. The white solid was purified by flash chromatography on silica gel.

6.3.1 N-Phenyl-4-(2-oxoimidazolidin-1-yl)benzenesulfonamide (8). Flash chromatography (CH₂Cl₂ to CH₂Cl₂/AcOEt 0:1). Yield: 29%; White solid; mp: 262-264 °C; IR: 3434, 1686 cm⁻¹; ¹H NMR (DMSO-d₆ and a few drops of CDCl₃) δ 7.63-7.53 (m, 4H, Ar), 7.11-7.02 (m, 4H, Ar), 6.95-6.88 (m, 1H, Ar), 3.82-3.78 (m, 2H, CH₂), 3.44-3.39 (m, 2H, CH₂); ¹³C NMR (DMSO-d₆ and CDCl₃) δ 158.3, 143.9, 137.5, 131.3, 128.5, 127.4, 123.4, 119.8, 115.8, 44.0, 36.3; HRMS (ES⁺) *m/z* found 318.0634; C₁₅H₁₅N₃O₃S (M⁺ + H) requires 318.0912.

6.3.2 N-2-Tolyl-4-(2-oxoimidazolidin-1-yl)benzenesulfonamide (9). Flash chromatography (CH₂Cl₂ to CH₂Cl₂/AcOEt 0:1). Yield: 45%; White solid; mp: 209-210 °C; IR: 3234, 2920, 1694 cm⁻¹; ¹H NMR (CDCl₃ and a few drops of CD₃OD and DMSO-d₆) δ 7.55-7.49 (m, 4H, Ar), 6.97-6.94 (m, 4H, Ar), 3.86-3.80 (m, 2H, CH₂), 3.48-3.42 (m, 2H, CH₂), 1.95 (s, 3H, CH₃); ¹³C NMR (CDCl₃, and a few drops of CD₃OD and DMSO-d₆) δ 158.8, 143.9, 134.6, 133.7, 132.5, 130.4, 127.5, 126.0, 126.0, 126.0, 116.1, 44.4, 36.5, 17.4; HRMS (ES⁺) *m/z* found 331.9980; C₁₆H₁₇N₃O₃S (M⁺ + H) requires 332.1069.

6.3.3 N-(2-Ethylphenyl)-4-(2-oxoimidazolidin-1-yl)benzenesulfonamide (10). Flash chromatography (CH₂Cl₂ to CH₂Cl₂/AcOEt 0:1). Yield: 40%; White solid; mp: 171-172 °C; IR: 3240, 2973, 1698 cm⁻¹; ¹H NMR (CDCl₃ and a few drops of CD₃OD) δ 7.62-7.45 (m, 4H, Ar), 7.06-6.80 (m, 4H, Ar), 3.84-3.76 (m, 2H, CH₂), 3.50-3.45 (m, 2H, CH₂), 2.36 (q, 2H, J = 7.5 Hz, CH₂), 0.95 (t, 3H, J = 7.5 Hz, CH₃); ¹³C NMR (CDCl₃ and few drops of CD₃OD) δ 159.4, 144.0, 138.7, 133.8, 132.5, 128.9, 128.1, 126.6, 126.4, 125.3, 116.6, 44.8, 36.9, 23.5, 14.1; HRMS (ES⁺) *m/z* found 346.0042; C₁₇H₁₉N₃O₃S (M⁺ + H) requires 346.1225.

6.3.4 N-(2-Methoxyphenyl)-4-(2-oxoimidazolidin-1-yl)benzenesulfonamide (11). Flash chromatography (CH₂Cl₂ to CH₂Cl₂/AcOEt 0:1). Yield: 53%; White solid; mp: 209-211 °C; IR: 3279, 2906, 1697 cm⁻¹; ¹H NMR (CDCl₃, and a few drops of CD₃OD and DMSO-d₆) δ 7.58-7.51 (m, 4H, Ar), 7.29 (d, 1H, J = 7.8 Hz, Ar), 6.96 (t, 1H, J = 7.8 Hz, Ar), 6.79-6.69 (m,

2H, Ar), 3.81-3.78 (m, 2H, CH₂), 3.52 (s, 3H, CH₃), 3.45-3.40 (m, 2H, CH₂); ¹³C NMR (CDCl₃, and a few drops of CD₃OD and DMSO-d₆) δ 158.4, 150.6, 144.0, 131.5, 127.5, 125.5, 125.4, 122.5, 120.2, 115.7, 110.8, 55.2, 44.2, 36.3; HRMS (ES+) *m/z* found 347.9580; C₁₆H₁₇N₃O₄S (M⁺ + H) requires 348.1018.

6.3.5 *N*-(2,3-Dimethylphenyl)-4-(2-oxoimidazolidin-1-yl)benzenesulfonamide (12). Flash chromatography (CH₂Cl₂ to CH₂Cl₂/AcOEt 0:1). Yield: 55%; White solid; mp: 231-232 °C; IR: 3257, 2902, 1703 cm⁻¹; ¹H NMR (DMSO-d₆ and a few drops of CDCl₃) δ 8.87 (s, 1H, NH), 7.57-7.49 (m, 4H, Ar), 6.90-6.80 (m, 3H, Ar and NH), 6.74-6.71 (m, 1H, Ar), 3.86-3.81 (m, 2H, CH₂), 3.49-3.43 (m, 2H, CH₂), 2.12 (s, 3H, CH₃), 1.92 (s, 3H, CH₃); ¹³C NMR (DMSO-d₆ and a few drops of CDCl₃) δ 158.4, 143.6, 137.0, 134.3, 133.2, 132.3, 127.5, 127.3, 124.8, 124.2, 115.6, 44.1, 36.3, 20.0, 13.6; HRMS (ES+) *m/z* found 346.1540; C₁₇H₁₉N₃O₃S (M⁺ + H) requires 346.1225.

6.3.6 *N*-(2,4-Dimethylphenyl)-4-(2-oxoimidazolidin-1-yl)benzenesulfonamide (13). Flash chromatography (CH₂Cl₂ to CH₂Cl₂/AcOEt 0:1). Yield: 55%; White solid; mp: 238-239 °C; IR: 3463, 3283, 1704 cm⁻¹; ¹H NMR (CDCl₃ and a few drops of DMSO-d₆) δ 8.86 (s, 1H, NH), 7.58-7.48 (m, 4H, Ar), 6.93 (s, 1H, NH), 6.82-6.74 (m, 3H, Ar), 3.87-3.81 (m, 2H, CH₂), 3.48-3.43 (m, 2H, CH₂), 2.16 (s, 3H, CH₃), 1.93 (s, 3H, CH₃); ¹³C NMR (CDCl₃ and a few drops of DMSO-d₆) δ 158.3, 143.7, 135.3, 133.8, 132.4, 131.9, 130.8, 127.2, 126.3, 115.6, 44.1, 36.3, 20.3, 17.3; HRMS (ES+) *m/z* found 345.9970; C₁₇H₁₉N₃O₃S (M⁺ + H) requires 346.1225.

6.3.7 *N*-(2,5-Dimethylphenyl)-4-(2-oxoimidazolidin-1-yl)benzenesulfonamide (14). Flash chromatography (CH₂Cl₂ to CH₂Cl₂/AcOEt 0:1). Yield: 46%; White solid; mp: 213-215 °C; IR: 3274, 1695 cm⁻¹; ¹H NMR (DMSO-d₆ and a few drops of CDCl₃) δ 9.05 (s, 1H, NH), 7.61-7.50 (m, 4H, Ar), 7.08 (s, 1H, NH), 6.90-6.79 (m, 3H, Ar), 3.87-3.82 (m, 2H, CH₂),

3.47-3.42 (m, 2H, CH₂), 2.15 (s, 3H, CH₃), 1.89 (s, 3H, CH₃); ¹³C NMR (DMSO-d₆ and a few drops of CDCl₃) δ 158.2, 143.8, 134.9, 134.5, 132.4, 130.3, 130.0, 127.2, 126.6, 126.4, 115.6, 44.1, 36.3, 20.3, 17.0; HRMS (ES+) *m/z* found 346.0067; C₁₇H₁₉N₃O₃S (M⁺ + H) requires 346.1225.

6.3.8 N-3-Tolyl-4-(2-oxoimidazolidin-1-yl)benzenesulfonamide (15). Flash chromatography (CH₂Cl₂ to CH₂Cl₂/AcOEt 0:1). Yield: 64%; White solid; mp: 188-190 °C; IR: 3419, 3077, 1697 cm⁻¹; ¹H NMR (DMSO-d₆ and a few drops of CDCl₃) δ 9.60 (s, 1H, NH), 7.63-7.52 (m, 4H, Ar), 6.97-6.92 (m, 1H, Ar), 6.84-6.82 (m, 2H, Ar or NH), 6.75-6.70 (m, 2H, Ar or NH), 3.83-3.77 (m, 2H, CH₂), 3.46-3.41 (m, 2H, CH₂), 2.15 (s, 3H, CH₃); ¹³C NMR (DMSO-d₆ and a few drops of CDCl₃) δ 158.3, 143.6, 138.0, 137.3, 131.5, 128.1, 127.3, 124.2, 120.4, 116.8, 115.7, 44.1, 36.3, 20.8; HRMS (ES+) *m/z* found 332.1365; C₁₆H₁₇N₃O₃S (M⁺ + H) requires 332.1069.

6.3.9 N-(3-Ethylphenyl)-4-(2-oxoimidazolidin-1-yl)benzenesulfonamide (16). Flash chromatography (CH₂Cl₂ to CH₂Cl₂/AcOEt 0:1 to AcOEt/MeOH 95:5). Yield: 72%; White solid; mp: 188-190 °C; IR: 3400, 2961, 1697 cm⁻¹; ¹H NMR (DMSO-d₆) δ 10.08 (s, 1H, NH), 7.69 (brs, 4H, Ar), 7.26 (brs, 1H, NH), 7.14-7.09 (m, 1H, Ar), 6.95-6.84 (m, 3H, Ar), 3.87-3.82 (m, 2H, CH₂), 3.43-3.38 (m, 2H, CH₂), 2.49 (q, 2H, J = 7.5 Hz, CH₂), 1.09 (t, 3H, J = 7.5 Hz, CH₃); ¹³C NMR (DMSO-d₆) δ 158.4, 144.7, 144.4, 138.0, 131.3, 129.0, 127.7, 123.3, 119.1, 117.1, 116.2, 44.2, 36.4, 28.1, 15.4; HRMS (ES+) *m/z* found 346.1010; C₁₇H₁₉N₃O₃S (M⁺ + H) requires 346.1225.

6.3.10 N-(3-Methoxyphenyl)-4-(2-oxoimidazolidin-1-yl)benzenesulfonamide (17). Flash chromatography (AcOEt to AcOEt/MeOH 95:5). Yield: 52%; White solid; mp: 179-181 °C; IR: 3428, 3084, 1700 cm⁻¹; ¹H NMR (DMSO-d₆) δ 10.17 (brs, 1H, NH), 7.70 (brs, 4H, Ar), 7.26 (brs, 1H, NH), 7.14-7.09 (m, 1H, Ar), 6.68-6.67 (m, 2H, Ar), 6.60-6.56 (m, 1H, Ar),

3.88-3.83 (m, 2H, CH₂), 3.66 (s, 3H, CH₃), 3.43-3.38 (m, 2H, CH₂); ¹³C NMR (DMSO-d₆) δ 159.7, 158.4, 144.4, 139.3, 131.1, 130.0, 127.7, 116.2, 111.7, 108.8, 105.5, 55.0, 44.2, 36.4; HRMS (ES⁺) *m/z* found 348.0766; C₁₆H₁₇N₃O₄S (M⁺ + H) requires 348.1018.

6.3.11 *N*-(3-Phenoxyphenyl)-4-(2-Oxoimidazolidin-1-yl)benzenesulfonamide (18). Flash chromatography (CH₂Cl₂ to CH₂Cl₂/AcOEt 0:1). Yield: 65%; White solid; mp: 208-211 °C; IR: 3389, 1696 cm⁻¹; ¹H NMR (DMSO-d₆) δ 10.26 (brs, 1H, NH), 7.73-7.63 (m, 4H, Ar), 7.43-7.37 (m, 2H, Ar), 7.31 (brs, 1H, NH), 7.26-7.15 (m, 2H, Ar), 6.93-6.86 (m, 3H, Ar), 6.73-6.64 (m, 2H, Ar), 3.91-3.86 (m, 2H, CH₂), 3.47-3.41 (m, 2H, CH₂); ¹³C NMR (DMSO-d₆) δ 158.4, 157.3, 156.1, 144.6, 139.6, 130.8, 130.6, 130.1, 127.8, 123.8, 118.9, 116.3, 114.5, 113.7, 109.4, 44.3, 36.4; HRMS (ES⁺) *m/z* found 410.1010; C₂₁H₁₉N₃O₄S (M⁺ + H) requires 410.1175.

6.3.12 *N*-(3-Bromophenyl)-4-(2-oxoimidazolidin-1-yl)benzenesulfonamide (19). Flash chromatography (CH₂Cl₂ to CH₂Cl₂/AcOEt 0:1). Yield: 21%; White solid; mp: 184-185 °C; IR: 3388, 2860, 1692 cm⁻¹; ¹H NMR (DMSO-d₆) δ 10.45 (brs, 1H, NH), 7.72 (s, 4H, Ar), 7.29-7.20 (m, 4H, Ar and NH), 7.14-7.10 (m, 1H, Ar), 3.90-3.84 (m, 2H, CH₂), 3.44-3.39 (m, 2H, CH₂); ¹³C NMR ((CD₃)₂CO and few drops of DMSO-d₆ and CDCl₃) δ 158.5, 144.7, 139.9, 131.3, 130.5, 127.7, 126.2, 122.1, 121.9, 118.2, 116.1, 44.3, 36.5; HRMS (ES⁺) *m/z* found 395.9071; C₁₅H₁₄BrN₃O₃S (M⁺ + H) requires 396.0018.

6.3.13 *N*-(3-Chlorophenyl)-4-(2-oxoimidazolidin-1-yl)benzenesulfonamide (20). Flash chromatography (CH₂Cl₂ to CH₂Cl₂/AcOEt 0:1). Yield: 30%; White solid; mp: 180-182 °C; IR: 3386, 1696 cm⁻¹; ¹H NMR (CDCl₃ and a few drops of CD₃OD and DMSO-d₆) δ 7.64-7.55 (m, 4H, Ar), 7.07-7.05 (m, 2H, Ar), 6.97-6.94 (m, 1H, Ar), 6.89-6.86 (m, 1H, Ar), 3.84-3.78 (m, 2H, CH₂), 3.45-3.40 (m, 2H, CH₂); ¹³C NMR (CDCl₃ and a few drops of CD₃OD and

DMSO- d_6) δ 158.7, 144.3, 139.2, 133.9, 131.3, 130.0, 127.7, 123.5, 119.4, 117.8, 116.2, 44.4, 36.5; HRMS (ES⁺) m/z found 352.0504; C₁₅H₁₄ClN₃O₃S (M⁺ + H) requires 352.0523.

6.3.14 *N*-(3,4-Dimethylphenyl)-4-(2-oxoimidazolidin-1-yl)benzenesulfonamide (21). Flash chromatography (AcOEt to AcOEt/MeOH 95:5). Yield: 73%; White solid; mp: 206-208 °C; IR: 3413, 3256, 1700 cm⁻¹; ¹H NMR (DMSO- d_6) δ 9.92 (s, 1H, NH), 7.70-7.63 (m, 4H, Ar), 7.26 (s, 1H, NH), 6.97-6.94 (m, 1H, Ar), 6.88-6.87 (m, 1H, Ar), 6.83-6.80 (m, 1H, Ar), 3.88-3.83 (m, 2H, CH₂), 3.43-3.39 (m, 2H, CH₂), 2.11 (s, 3H, CH₃), 2.09 (s, 3H, CH₃); ¹³C NMR (DMSO- d_6) δ 158.4, 144.3, 136.8, 135.6, 131.8, 131.4, 129.9, 127.7, 121.5, 117.6, 116.2, 44.2, 36.4, 19.6, 18.6; HRMS (ES⁺) m/z found 346.0768; C₁₇H₁₉N₃O₃S (M⁺ + H) requires 346.1225.

6.3.15 *N*-(3,5-Dimethylphenyl)-4-(2-oxoimidazolidin-1-yl)benzenesulfonamide (22). Flash chromatography (CH₂Cl₂ to CH₂Cl₂/AcOEt 0:1). Yield: 68%; White solid; mp: 216-218 °C; IR: 3406, 1699 cm⁻¹; ¹H NMR (DMSO- d_6 and a few drops of CDCl₃) δ 9.66 (s, 1H, NH), 7.64-7.54 (m, 4H, Ar), 6.97 (s, 1H, NH), 6.66 (s, 2H, Ar), 6.54 (s, 1H, Ar), 3.84-3.79 (m, 2H, CH₂), 3.45-3.40 (m, 2H, CH₂), 2.11 (s, 6H, 2x CH₃); ¹³C NMR (DMSO- d_6 and a few drops of CDCl₃) δ 158.3, 143.8, 137.7, 137.4, 131.5, 127.3, 125.0, 117.3, 115.7, 44.0, 36.3, 20.7; HRMS (ES⁺) m/z found 346.0776; C₁₇H₁₉N₃O₃S (M⁺ + H) requires 346.1225.

6.3.16 *N*-(3,5-Di-*tert*-butylphenyl)-4-(2-oxoimidazolidin-1-yl)benzenesulfonamide (23). Flash chromatography (CH₂Cl₂ to CH₂Cl₂/AcOEt 0:1 to AcOEt/MeOH 95:5). Yield: 86%; White solid; mp: 276-278 °C; IR: 3400, 3107, 1703 cm⁻¹; ¹H NMR (DMSO- d_6) δ 9.95 (s, 1H, NH), 7.73-7.66 (m, 4H, Ar), 7.27 (brs, 1H, NH), 7.04 (s, 1H, Ar), 6.95-6.93 (m, 2H, Ar), 3.88-3.83 (m, 2H, CH₂), 3.45-3.40 (m, 2H, CH₂), 1.20 (s, 18H, 6x CH₃); ¹³C NMR (DMSO- d_6) δ 158.4, 151.0, 144.4, 137.4, 131.4, 127.8, 117.3, 116.1, 114.3, 44.3, 36.3, 34.5, 31.1; HRMS (ES⁺) m/z found 430.2245; C₂₃H₃₁N₃O₃S (M⁺ + H) requires 430.2164.

6.3.17 *N*-(3,4-Difluorophenyl)-4-(2-oxoimidazolidin-1-yl)benzenesulfonamide (24). Flash chromatography (CH₂Cl₂ to CH₂Cl₂/AcOEt 0:1). Yield: 37%; White solid; mp: 225-226 °C; IR: 3430, 3129, 1695 cm⁻¹; ¹H NMR (CDCl₃ and a few drops of CD₃OD and DMSO-d₆) δ 7.62-7.53 (m, 4H, Ar), 6.99-6.87 (m, 2H, Ar), 6.79-6.74 (m, 1H, Ar), 3.86-3.80 (m, 2H, CH₂), 3.48-3.43 (m, 2H, CH₂); ¹³C NMR (CDCl₃ and a few drops of CD₃OD and DMSO-d₆) δ 158.7, 151.2, 151.0, 148.4, 148.2, 147.9, 147.7, 145.2, 145.0, 144.0, 134.2, 134.1, 134.1, 134.0, 130.9, 127.5, 117.0, 116.8, 116.5, 116.4, 116.4, 116.3, 116.1, 109.9, 109.6, 44.3, 36.4; HRMS (ES⁺) *m/z* found 354.0279; C₁₅H₁₃F₂N₃O₃S (M⁺ + H) requires 354.0724.

6.3.18 *N*-(3,4-Dimethoxyphenyl)-4-(2-oxoimidazolidin-1-yl)benzenesulfonamide (25). Flash chromatography (CH₂Cl₂ to CH₂Cl₂/AcOEt 0:1 to AcOEt/MeOH 95:5). Yield: 59%; Brownish solid; mp: 215-216 °C; IR: 3357, 3111, 1701 cm⁻¹; ¹H NMR (DMSO-d₆) δ 9.80 (brs, 1H, NH), 7.71-7.63 (m, 4H, Ar), 7.27 (brs, 1H, NH), 6.81-6.78 (m, 1H, Ar), 6.73-6.72 (m, 1H, Ar), 6.58-6.54 (m, 1H, Ar), 3.90-3.84 (m, 2H, CH₂), 3.67 (s, 3H, CH₃), 3.66 (s, 3H, CH₃), 3.45-3.40 (m, 2H, CH₂); ¹³C NMR (DMSO-d₆) δ 158.4, 148.8, 145.9, 144.3, 131.2, 131.0, 127.8, 116.1, 113.2, 112.1, 106.3, 55.6, 55.4, 44.3, 36.4; HRMS (ES⁺) *m/z* found 378.0635; C₁₇H₁₉N₃O₅S (M⁺ + H) requires 378.1123.

6.3.19 *N*-(3,5-Dimethoxyphenyl)-4-(2-oxoimidazolidin-1-yl)benzenesulfonamide (26). Flash chromatography (CH₂Cl₂ to CH₂Cl₂/AcOEt 0:1). Yield: 43%; White solid; mp: 200-201 °C; IR: 3434, 3178, 1702 cm⁻¹; ¹H NMR (CDCl₃ and a few drops of CD₃OD and DMSO-d₆) δ 7.67-7.56 (m, 4H, Ar), 6.25-6.24 (m, 2H, Ar), 6.01-6.00 (m, 1H, Ar), 3.83-3.78 (m, 2H, CH₂), 3.60 (s, 6H, 2x CH₃), 3.44-3.38 (m, 2H, CH₂); ¹³C NMR (CDCl₃ and a few drops of CD₃OD and DMSO-d₆) δ 160.5, 158.3, 144.0, 139.3, 131.2, 127.5, 115.9, 97.5, 95.0, 54.6, 44.0, 36.2; HRMS (ES⁺) *m/z* found 378.0471; C₁₇H₁₉N₃O₅S (M⁺ + H) requires 378.1124.

6.3.20 N-(3,4,5-Trimethoxyphenyl)-4-(2-oxoimidazolidin-1-yl)benzenesulfonamide (27).

Flash chromatography (AcOEt to AcOEt/MeOH 95:5). Yield: 23%; White solid; mp: 233-235 °C; IR: 3416, 3120, 1704 cm^{-1} ; ^1H NMR (DMSO- d_6) δ 10.31 (brs, 1H, NH), 7.72 (s, 4H, Ar), 7.27 (s, 1H, NH), 6.41 (s, 2H, Ar), 3.90-3.85 (m, 2H, CH_2), 3.67 (s, 6H, 2x CH_3), 3.57 (s, 3H, CH_3), 3.45-3.40 (m, 2H, CH_2); ^{13}C NMR (DMSO- d_6) δ 158.4, 153.0, 144.5, 134.0, 133.9, 131.1, 127.9, 116.2, 97.6, 60.1, 55.8, 44.2, 36.4; HRMS (ES+) m/z found 408.0733; $\text{C}_{18}\text{H}_{21}\text{N}_3\text{O}_6\text{S}$ ($\text{M}^+ + \text{H}$) requires 408.1229.

6.3.21 N-4-Tolyl-4-(2-oxoimidazolidin-1-yl)benzenesulfonamide (28).

Flash chromatography (CH_2Cl_2 to $\text{CH}_2\text{Cl}_2/\text{AcOEt}$ 0:1 to AcOEt/MeOH 95:5). Yield: 83%; White solid; mp: 218-220 °C; IR: 3430, 1697 cm^{-1} ; ^1H NMR (DMSO- d_6) δ 9.97 (brs, 1H, NH), 7.70-7.63 (m, 4H, Ar), 7.26 (brs, 1H, NH), 7.04-6.96 (m, 4H, Ar), 3.88-3.82 (m, 2H, CH_2), 3.44-3.38 (m, 2H, CH_2), 2.19 (s, 3H, CH_3); ^{13}C NMR (DMSO- d_6) δ 158.4, 144.3, 135.3, 133.1, 131.2, 129.5, 127.7, 120.4, 116.2, 44.2, 36.4, 20.3; HRMS (ES+) m/z found 332.1114; $\text{C}_{16}\text{H}_{17}\text{N}_3\text{O}_3\text{S}$ ($\text{M}^+ + \text{H}$) requires 332.1069.

6.3.22 N-(4-Ethylphenyl)-4-(2-oxoimidazolidin-1-yl)benzenesulfonamide (29).

Flash chromatography (CH_2Cl_2 to $\text{CH}_2\text{Cl}_2/\text{AcOEt}$ 0:1 to AcOEt/MeOH 95:5). Yield: 65%; White solid; mp: 195-196 °C; IR: 3250, 1695 cm^{-1} ; ^1H NMR (CDCl_3 and a few drops of CD_3OD and DMSO- d_6) δ 7.61-7.50 (m, 4H, Ar), 6.95-6.89 (m, 4H, Ar), 3.81-3.76 (m, 2H, Ar), 3.45-3.39 (m, 2H, CH_2), 2.44 (q, 2H, $J = 7.6$ Hz, CH_2), 1.06 (t, 3H, $J = 7.6$ Hz, CH_3); ^{13}C NMR (CDCl_3 and a few drops of CD_3OD and DMSO- d_6) δ 158.7, 143.9, 139.9, 134.9, 131.8, 128.0, 127.7, 120.8, 116.1, 44.4, 36.5, 27.7, 15.2; HRMS (ES+) m/z found 346.0152; $\text{C}_{17}\text{H}_{19}\text{N}_3\text{O}_3\text{S}$ ($\text{M}^+ + \text{H}$) requires 346.1225.

6.3.24 N-(4-Butylphenyl)-4-(2-oxoimidazolidin-1-yl)benzenesulfonamide (30).

Flash chromatography (CH_2Cl_2 to $\text{CH}_2\text{Cl}_2/\text{AcOEt}$ 0:1 to AcOEt/MeOH 95:5). Yield: 81%; White

solid; mp: 203-205 °C; IR: 3436, 2927, 1692 cm^{-1} ; ^1H NMR (DMSO- d_6) δ 10.00 (s, 1H, NH), 7.70-7.64 (m, 4H, Ar), 7.26 (s, 1H, NH), 7.06-6.98 (m, 4H, Ar), 3.89-3.83 (m, 2H, CH_2), 3.44-3.39 (m, 2H, CH_2), 2.49-2.44 (m, 2H, CH_2), 1.52-1.42 (m, 2H, CH_2), 1.31-1.19 (m, 2H, CH_2), 0.87 (t, 3H, $J = 7.3$ Hz, CH_3); ^{13}C NMR (DMSO- d_6) δ 158.4, 144.3, 138.0, 135.5, 131.4, 128.9, 127.7, 120.3, 116.2, 44.3, 36.4, 34.1, 33.1, 21.7, 13.8; HRMS (ES+) m/z found 374.1300; $\text{C}_{19}\text{H}_{23}\text{N}_3\text{O}_3\text{S}$ ($\text{M}^+ + \text{H}$) requires 374.1538.

6.3.25 *N*-(4-*sec*-Butylphenyl)-4-(2-oxoimidazolidin-1-yl)benzenesulfonamide (31). Flash chromatography (AcOEt to AcOEt/MeOH 95:5). Yield: 69%; White solid; mp: 157-159 °C; IR: 3436, 2960, 1690 cm^{-1} ; ^1H NMR (DMSO- d_6) δ 10.01 (s, 1H, NH), 7.71-7.65 (m, 4H, Ar), 7.26 (s, 1H, NH), 7.06-6.98 (m, 4H, Ar), 3.88-3.83 (m, 2H, CH_2), 3.44-3.38 (m, 2H, CH_2), 2.49-2.44 (m, 1H, CH), 1.51-1.41 (m, 2H, CH_2), 1.11 (d, 3H, $J = 7.0$ Hz, CH_3), 0.70 (t, 3H, $J = 7.3$ Hz, CH_3); ^{13}C NMR (DMSO- d_6) δ 158.4, 144.3, 142.7, 135.6, 131.5, 127.7, 127.5, 120.2, 116.2, 44.2, 40.1, 36.4, 30.6, 21.5, 12.0; HRMS (ES+) m/z found 374.1019; $\text{C}_{19}\text{H}_{23}\text{N}_3\text{O}_3\text{S}$ ($\text{M}^+ + \text{H}$) requires 374.1538.

6.3.26 *N*-(4-*tert*-Butylphenyl)-4-(2-oxoimidazolidin-1-yl)benzenesulfonamide (32). Flash chromatography (CH_2Cl_2 to $\text{CH}_2\text{Cl}_2/\text{AcOEt}$ 0:1 to AcOEt/MeOH 95:5). Yield: 84%; White solid; mp: 241-243 °C; IR: 3357, 3112, 1694 cm^{-1} ; ^1H NMR (DMSO- d_6) δ 10.06 (s, 1H, NH), 7.70 (s, 4H, Ar), 7.26-7.23 (m, 3H, NH and Ar), 7.02-7.00 (m, 2H, Ar), 3.89-3.84 (m, 2H, CH_2), 3.44-3.39 (m, 2H, CH_2), 1.20 (s, 9H, 3x CH_3); ^{13}C NMR (DMSO- d_6) δ 158.4, 146.1, 144.3, 135.3, 131.6, 127.7, 125.8, 119.7, 116.3, 44.2, 36.4, 34.0, 31.1; HRMS (ES+) m/z found 374.0975; $\text{C}_{19}\text{H}_{23}\text{N}_3\text{O}_3\text{S}$ ($\text{M}^+ + \text{H}$) requires 374.1538.

6.3.27 *N*-(4-Pentylphenyl)-4-(2-oxoimidazolidin-1-yl)benzenesulfonamide (33). Flash chromatography (CH_2Cl_2 to $\text{CH}_2\text{Cl}_2/\text{AcOEt}$ 0:1 to AcOEt/MeOH 95:5). Yield: 82%; White solid; mp: 207-209 °C; IR: 3314, 2927, 1705 cm^{-1} ; ^1H NMR (DMSO- d_6) δ 9.98 (brs, 1H, NH),

7.69-7.63 (m, 4H, Ar), 7.25 (brs, 1H, NH), 7.04-6.96 (m, 4H, Ar), 3.87-3.81 (m, 2H, CH₂), 3.43-3.37 (m, 2H, CH₂), 2.44 (t, 2H, J = 7.5 Hz, CH₂), 1.52-1.45 (m, 2H, CH₂), 1.30-1.18 (m, 4H, 2x CH₂), 0.83 (t, 3H, J = 6.8 Hz, CH₃); ¹³C NMR (DMSO-d₆) δ 158.4, 144.3, 138.0, 135.5, 131.3, 128.8, 127.7, 120.3, 116.2, 44.2, 36.4, 34.4, 30.9, 30.5, 21.9, 13.9; HRMS (ES+) *m/z* found 388.1610; C₂₀H₂₅N₃O₃S (M⁺ + H) requires 388.1695.

6.3.28 *N*-(4-Cyclohexylphenyl)-4-(2-oxoimidazolidin-1-yl)benzenesulfonamide (34). Flash chromatography (CH₂Cl₂ to CH₂Cl₂/AcOEt 0:1 to AcOEt/MeOH 95:5). Yield: 35%; White solid; mp: 256-257 °C; IR: 3287, 2927, 1708 cm⁻¹; ¹H NMR (DMSO-d₆) δ 10.04 (s, 1H, NH), 7.69 (s, 4H, Ar), 7.27 (s, 1H, NH), 7.09-6.98 (m, 4H, Ar), 3.89-3.84 (m, 2H, CH₂), 3.44-3.39 (m, 2H, CH₂), 2.42-2.35 (m, 1H, CH), 1.76-1.66 (m, 5H, 5x CHequ), 1.36-1.16 (m, 5H, 5x CHax); ¹³C NMR (DMSO-d₆) δ 158.4, 144.3, 143.2, 135.7, 131.5, 127.7, 127.2, 120.1, 116.2, 44.3, 43.0, 36.4, 33.9, 26.3, 25.6; HRMS (ES+) *m/z* found 400.1554; C₂₁H₂₅N₃O₃S (M⁺ + H) requires 400.1695.

6.3.29 *N*-(4-Heptylphenyl)-4-(2-oxoimidazolidin-1-yl)benzenesulfonamide (35). Flash chromatography (CH₂Cl₂ to CH₂Cl₂/AcOEt 0:1 to AcOEt/MeOH 95:5). Yield: 90%; White solid; mp: 188-190 °C; IR: 3250, 2924, 1710 cm⁻¹; ¹H NMR (DMSO-d₆) δ 9.99 (s, 1H, NH), 7.70-7.63 (m, 4H, Ar), 7.26 (s, 1H, NH), 7.05-6.97 (m, 4H, Ar), 3.88-3.83 (m, 2H, CH₂), 3.44-3.38 (m, 2H, CH₂), 2.45 (t, 2H, J = 7.6 Hz, CH₂), 1.50-1.46 (m, 2H, CH₂), 1.28-1.19 (m, 8H, 4x CH₂), 0.85 (t, 3H, J = 6.5 Hz, CH₃); ¹³C NMR (DMSO-d₆) δ 158.4, 144.3, 138.0, 135.5, 131.3, 128.8, 127.7, 120.3, 116.2, 44.2, 36.4, 34.4, 31.2, 30.9, 28.6, 28.5, 22.1, 13.9; HRMS (ES+) *m/z* found 416.0854; C₂₂H₂₉N₃O₃S (M⁺ + H) requires 416.2008.

6.3.30 *N*-(4-Methoxyphenyl)-4-(2-oxoimidazolidin-1-yl)benzenesulfonamide (36). Flash chromatography (CH₂Cl₂ to CH₂Cl₂/AcOEt 0:1). Yield: 68%; White solid; mp: 210-211 °C; IR: 3268, 3109, 1694 cm⁻¹; ¹H NMR (CDCl₃ and a few drops of CD₃OD and DMSO-d₆) δ

9.30 (s, 1H, NH), 7.56-7.49 (m, 4H, Ar), 6.93-6.90 (m, 2H, Ar), 6.75 (s, 1H, NH), 6.63-6.60 (m, 2H, Ar), 3.83-3.77 (m, 2H, CH₂), 3.62 (s, 3H, CH₃), 3.46-3.40 (m, 2H, CH₂); ¹³C NMR (CDCl₃ and a few drops of CD₃OD and DMSO-d₆) δ 158.4, 156.3, 143.6, 129.9, 127.4, 123.4, 123.4, 115.7, 113.6, 54.7, 44.1, 36.4; HRMS (ES⁺) *m/z* found 347.9559; C₁₆H₁₇N₃O₄S (M⁺ + H) requires 348.1018.

6.3.31 *N*-(4-Butoxyphenyl)-4-(2-oxoimidazolidin-1-yl)benzenesulfonamide (37). Flash chromatography (CH₂Cl₂ to CH₂Cl₂/AcOEt 0:1 to AcOEt/MeOH 95:5). Yield: 77%; White solid; mp: 223-225 °C; IR: 3270, 2954, 1693 cm⁻¹; ¹H NMR (DMSO-d₆) δ 9.77 (s, 1H, NH), 7.70-7.59 (m, 4H, Ar), 7.27 (s, 1H, NH), 6.99-6.96 (m, 2H, Ar), 6.81-6.78 (m, 2H, Ar), 3.89-3.85 (m, 4H, 2x CH₂), 3.45-3.40 (m, 2H, CH₂), 1.70-1.60 (m, 2H, CH₂), 1.47-1.35 (m, 2H, CH₂), 0.92 (t, 3H, J = 7.4 Hz, CH₃); ¹³C NMR (DMSO-d₆) δ 158.4, 155.9, 144.2, 131.2, 130.4, 127.7, 123.2, 116.1, 114.8, 67.2, 44.3, 36.4, 30.8, 18.7, 13.7; HRMS (ES⁺) *m/z* found 390.1243; C₁₉H₂₃N₃O₄S (M⁺ + H) requires 390.1487.

6.3.32 *N*-(4-Hexyloxyphenyl)-4-(2-oxoimidazolidin-1-yl)benzenesulfonamide (38). Flash chromatography (CH₂Cl₂ to CH₂Cl₂/AcOEt 0:1). Yield: 41%; White solid; mp: 225-226 °C; IR: 3272, 2928, 1694 cm⁻¹; ¹H NMR (DMSO-d₆) δ 9.74 (s, 1H, NH), 7.67-7.56 (m, 4H, Ar), 7.24 (s, 1H, NH), 6.96-6.93 (m, 2H, Ar), 6.78-6.75 (m, 2H, Ar), 3.86-3.81 (m, 4H, 2x CH₂), 3.42-3.37 (m, 2H, CH₂), 1.68-1.58 (m, 2H, CH₂), 1.37-1.24 (m, 6H, 3x CH₂), 0.85 (t, 3H, J = 6.6 Hz, CH₃); ¹³C NMR (DMSO-d₆) δ 158.3, 155.8, 144.2, 131.1, 130.2, 127.6, 123.1, 116.0, 114.7, 67.5, 44.2, 36.3, 30.9, 28.6, 25.1, 22.0, 13.8; HRMS (ES⁺) *m/z* found 418.1668; C₂₁H₂₇N₃O₄S (M⁺ + H) requires 418.1801.

6.3.33 *N*-(4-Bromophenyl)-4-(2-oxoimidazolidin-1-yl)benzenesulfonamide (39). Flash chromatography (AcOEt to AcOEt/MeOH 95:5). Yield: 57%; White solid; mp: 237-239 °C; IR: 3353, 3139, 1683 cm⁻¹; ¹H NMR (DMSO-d₆) δ 10.32 (s, 1H, NH), 7.72-7.66 (m, 4H, Ar),

7.42 (d, 2H, J = 8.7 Hz, Ar), 7.28 (s, 1H, NH), 7.05 (d, 2H, J = 8.7 Hz, Ar), 3.89-3.83 (m, 2H, CH₂), 3.44-3.38 (m, 2H, CH₂); ¹³C NMR (DMSO-d₆) δ 158.4, 144.6, 137.5, 132.0, 130.7, 127.7, 121.7, 116.3, 115.9, 44.2, 36.4; HRMS (ES⁺) *m/z* found 395.7357; C₁₅H₁₄BrN₃O₃S (M⁺ + H) requires 396.0018.

6.3.34 *N*-(4-Chlorophenyl)-4-(2-oxoimidazolidin-1-yl)benzenesulfonamide (**40**). Flash chromatography (AcOEt to AcOEt/MeOH 95:5). Yield: 47%; White solid; mp: 234-236 °C; IR: 3267, 1696 cm⁻¹; ¹H NMR (DMSO-d₆) δ 10.31 (s, 1H, NH), 7.72-7.65 (m, 4H, Ar), 7.31-7.28 (m, 3H, NH and Ar), 7.11-7.09 (m, 2H, Ar), 3.89-3.83 (m, 2H, CH₂), 3.48-3.38 (m, 2H, CH₂); ¹³C NMR (DMSO-d₆) δ 158.4, 144.6, 137.0, 130.8, 129.1, 127.9, 127.7, 121.4, 116.3, 44.2, 36.3; HRMS (ES⁺) *m/z* found 352.1068; C₁₅H₁₄ClN₃O₃S (M⁺ + H) requires 352.0522.

6.3.35 *N*-(4-Fluorophenyl)-4-(2-oxoimidazolidin-1-yl)benzenesulfonamide (**41**). Flash chromatography (CH₂Cl₂ to CH₂Cl₂/AcOEt 0:1). Yield: 68%; White solid; mp: 249-251 °C; IR: 3446, 3023, 1697 cm⁻¹; ¹H NMR (CDCl₃ and a few drops of CD₃OD and DMSO-d₆) δ 7.60-7.54 (m, 4H, Ar), 7.04-7.00 (m, 2H, Ar), 6.85-6.80 (m, 2H, Ar), 3.86-3.80 (m, 2H, CH₂), 3.47-3.42 (m, 2H, CH₂); ¹³C NMR (CDCl₃ and a few drops of CD₃OD and DMSO-d₆) δ 160.8, 158.5, 157.6, 144.0, 133.6, 133.5, 131.1, 127.5, 122.8, 122.7, 116.0, 115.3, 115.0, 44.2, 36.4; HRMS (ES⁺) *m/z* found 335.9753; C₁₅H₁₄FN₃O₃S (M⁺ + H) requires 336.0818.

6.3.36 *N*-(4-Iodophenyl)-4-(2-oxoimidazolidin-1-yl)benzenesulfonamide (**42**). Flash chromatography (AcOEt to AcOEt/MeOH 95:5). Yield: 53%; White solid; mp: 266-267 °C; IR: 3353, 3134, 1684 cm⁻¹; ¹H NMR (DMSO-d₆) δ 10.31 (brs, 1H, NH), 7.72-7.66 (m, 4H, Ar), 7.56 (d, 2H, J = 8,6 Hz, Ar), 7.28 (brs, 1H, NH), 6.92 (d, 2H, J = 8.6 Hz, Ar), 3.89-3.83 (m, 2H, CH₂), 3.44-3.39 (m, 2H, CH₂); ¹³C NMR (DMSO-d₆) δ 158.4, 144.6, 138.0, 137.8, 130.8, 127.7, 121.8, 116.3, 87.8, 44.2, 36.4; HRMS (ES⁺) *m/z* found 443.9131; C₁₅H₁₄IN₃O₃S (M⁺ + H) requires 443.9879.

6.3.37 N-(4-Cyanomethylphenyl)-4-(2-oxoimidazolidin-1-yl)benzenesulfonamide (43).

Flash chromatography (CH₂Cl₂ to CH₂Cl₂/AcOEt 0:1 to AcOEt/MeOH 95:5). Yield: 59%; Orange solid; mp: 204-206 °C; IR: 3298, 3136, 1699 cm⁻¹; ¹H NMR (DMSO-d₆) δ 10.25 (brs, 1H, NH), 7.74-7.70 (m, 4H, Ar), 7.27 (brs, 1H, NH), 7.23-7.11 (m, 4H, Ar), 3.92 (s, 2H, CH₂), 3.89-3.84 (m, 2H, CH₂), 3.44-3.39 (m, 2H, CH₂); ¹³C NMR (DMSO-d₆) δ 158.4, 144.5, 137.5, 131.0, 128.9, 127.7, 126.5, 120.2, 119.2, 116.3, 44.2, 36.4, 21.7; HRMS (ES⁺) *m/z* found 357.0658; C₁₇H₁₆N₄O₃S (M⁺ + H) requires 357.1021.

6.3.38 N-(4-Difluoromethoxyphenyl)-4-(2-oxoimidazolidin-1-yl)benzenesulfonamide (44).

Flash chromatography (CH₂Cl₂ to CH₂Cl₂/AcOEt 0:1 to AcOEt/MeOH 95:5). Yield: 81%; White solid; mp: 198-200 °C; IR: 3268, 3111, 1695 cm⁻¹; ¹H NMR (DMSO-d₆) δ 10.21 (brs, 1H, NH), 7.73-7.66 (m, 4H, Ar), 7.28 (brs, 1H, NH), 7.15-7.06 (m, 4H, Ar), 7.12 (t, 1H, J = 74.2 Hz, CHF₂), 3.90-3.85 (m, 2H, CH₂), 3.45-3.40 (m, 2H, CH₂); ¹³C NMR (DMSO-d₆) δ 158.4, 147.2, 144.5, 135.2, 131.0, 127.7, 121.7, 119.8, 116.4, 116.3, 44.2, 36.4; HRMS (ES⁺) *m/z* found 383.9433; C₁₆H₁₅F₂N₃O₄S (M⁺ + H) requires 384.0829.

6.3.39 N-Benzo[1,3]dioxol-5-yl-4-(2-oxoimidazolidin-1-yl)benzenesulfonamide (45).

Flash chromatography (CH₂Cl₂ to CH₂Cl₂/AcOEt 0:1). Yield: 54%; White solid; mp: 219-220 °C; IR: 3223, 2969, 1694 cm⁻¹; ¹H NMR (DMSO-d₆) δ 9.86 (brs, 1H, NH), 7.72-7.62 (m, 4H, Ar), 7.28 (brs, 1H, NH), 6.78-6.76 (m, 1H, Ar), 6.67-6.66 (m, 1H, Ar), 6.51-6.48 (m, 1H, Ar), 5.97 (s, 2H, CH₂), 3.90-3.85 (m, 2H, CH₂), 3.45-3.40 (m, 2H, CH₂); ¹³C NMR (DMSO-d₆) δ 158.4, 147.4, 144.4, 144.3, 131.8, 131.0, 127.7, 116.2, 114.5, 108.3, 103.2, 101.3, 44.3, 36.4; HRMS (ES⁺) *m/z* found 362.1037; C₁₆H₁₅N₃O₅S (M⁺ + H) requires 362.0811.

6.3.40 N-(9H-Fluoren-2-yl)-4-(2-oxoimidazolidin-1-yl)benzenesulfonamide (46).

Flash chromatography (CH₂Cl₂ to CH₂Cl₂/AcOEt 0:1 to AcOEt/MeOH 95:5). Yield: 38%; Orange solid; mp: 164-166 °C; IR: 3262, 1705 cm⁻¹; ¹H NMR (DMSO-d₆) δ 10.21 (brs, 1H, NH),

7.78-7.66 (m, 6H, Ar), 7.54-7.51 (m, 1H, Ar), 7.36-7.24 (m, 4H, Ar and NH), 7.14-7.11 (m, 1H, Ar), 3.84-3.80 (m, 4H, 2x CH₂), 3.41-3.37 (m, 2H, CH₂); ¹³C NMR (DMSO-d₆) δ 158.4, 144.4, 144.1, 142.7, 140.6, 137.2, 136.9, 131.2, 127.7, 126.8, 126.4, 125.0, 120.5, 119.6, 118.9, 117.0, 116.2, 44.2, 36.4, 36.3; HRMS (ES⁺) *m/z* found 406.0688; C₂₂H₁₉N₃O₃S (M⁺ + H) requires 406.1225.

6.3.41 *N-Indan-5-yl-4-(2-oxoimidazolidin-1-yl)benzenesulfonamide* (**47**). Flash chromatography (CH₂Cl₂ to CH₂Cl₂/AcOEt 0:1 to AcOEt/MeOH 95:5). Yield: 91%; White solid; mp: 228-230 °C; IR: 3251, 2964, 1694 cm⁻¹; ¹H NMR (DMSO-d₆) δ 9.97 (brs, 1H, NH), 7.71-7.65 (m, 4H, Ar), 7.27 (brs, 1H, NH), 7.07-7.04 (m, 1H, Ar), 6.98 (s, 1H, Ar), 6.87-6.84 (m, 1H, Ar), 3.89-3.84 (m, 2H, CH₂), 3.45-3.40 (m, 2H, CH₂), 2.78-2.72 (m, 4H, 2x CH₂), 2.00-1.90 (m, 2H, CH₂); ¹³C NMR (DMSO-d₆) δ 158.4, 144.6, 144.3, 139.4, 136.1, 131.4, 127.7, 124.5, 118.4, 116.5, 116.2, 44.3, 36.4, 32.4, 31.6, 25.1; HRMS (ES⁺) *m/z* found 358.0985; C₁₈H₁₉N₃O₃S (M⁺ + H) requires 358.1225.

6.3.42 *N-(1H-Indol-5-yl)-4-(2-oxoimidazolidin-1-yl)benzenesulfonamide* (**48**). Flash chromatography (CH₂Cl₂ to CH₂Cl₂/AcOEt 0:1 to AcOEt/MeOH 95:5). Yield: 82%; Reddish solid; mp: 239-241 °C; IR: 3372, 3252, 1960 cm⁻¹; ¹H NMR (DMSO-d₆) δ 11.04 (brs, 1H, NH), 9.68 (brs, 1H, NH), 7.67-7.59 (m, 4H, Ar), 7.31-7.30 (m, 1H, Ar), 7.25-7.22 (m, 3H, Ar), 6.86-6.83 (m, 1H, Ar), 6.34 (brs, 1H, NH), 3.86-3.81 (m, 2H, CH₂), 3.43-3.38 (m, 2H, CH₂); ¹³C NMR (DMSO-d₆) δ 158.4, 144.1, 133.6, 131.6, 129.3, 127.7, 127.7, 126.2, 117.0, 116.0, 113.6, 111.5, 101.1, 44.2, 36.4; HRMS (ES⁺) *m/z* found 357.0972; C₁₇H₁₆N₄O₃S (M⁺ + H) requires 357.1021.

6.4 Preparation of Compounds 49 to 51

6.4.1 1-(2-Chloroethyl)-3-phenylurea (**49**). 2-Chloroethylisocyanate (1.2 eq.) was added dropwise to a cold solution (ice bath) of aniline (1.0 eq.) in dry methylene chloride (15 mL

per g of aniline). The ice bath was removed and the reaction mixture was stirred at room temperature for 24 h. After completion of the reaction, the solvent was evaporated under reduced pressure to give a white solid, which was triturated twice with cold hexanes/ether 10:1. Yield: 99%; mp: 108-110 °C; IR ν : 3304, 1637 cm^{-1} ; ^1H NMR (DMSO- d_6): δ 8.69 (s, 1H, NH), 7.44-7.41 (m, 2H, Ar), 7.27-7.22 (m, 2H, Ar), 6.95-6.90 (m, 1H, Ar), 6.45 (t, 1H, J = 5.1 Hz, NH), 3.68 (t, 2H, J = 6.1 Hz, CH_2), 3.48-3.42 (m, 2H, CH_2); ^{13}C NMR (CDCl_3 and few drops of CD_3OD): δ 156.5, 138.9, 128.8, 122.7, 119.5, 44.0, 41.7.

6.4.2 1-Phenylimidazolidin-2-one (50). Sodium hydride (3 eq.) was slowly added to a cold solution of compound **49** (1 eq.) in tetrahydrofuran under dry nitrogen atmosphere. The ice bath was removed after 30 min and the reaction mixture was stirred at room temperature for 5 h. The reaction was quenched at 0 °C with water and diluted with ethyl acetate. The organic layer was washed with water and brine, dried over sodium sulfate, filtered, and concentrated *in vacuo* to provide **50**, which were used without further purification to afford white solids. Yield: 98%; Compound **50** was also synthesized using method described by Neville.[40] Briefly, triphosgene (12.2 mmol) was dissolved in 40 mL of tetrahydrofuran and cooled at 0°C. To the resulting solution was added (36.7 mmol) of *N*-phenylethylenediamine dissolved in 65 mL of tetrahydrofuran and 7.7 mL of triethylamine over a period of 30 min. A white solid immediately precipitated and the reaction was complete after 5 min. The reaction mixture was quenched with water and diluted with ethyl acetate. The organic layer was washed with water and brine, dried over sodium sulfate, filtered, and concentrated *in vacuo*. The residue was purified by flash chromatography (CH_2Cl_2 to $\text{CH}_2\text{Cl}_2/\text{AcOEt}$ 3:10) to afford a white solid. Yield: 80%; mp: 154-156 °C; IR ν : 3240, 1680 cm^{-1} ; ^1H NMR (DMSO- d_6): δ 7.58-7.55 (m, 2H, Ar), 7.34-7.29 (m, 2H, Ar), 7.02-6.95 (m, 2H, Ar and NH), 3.88-3.83 (m, 2H, CH_2), 3.44-3.39 (m, 2H, CH_2); ^{13}C NMR (CDCl_3): δ 160.2, 140.2, 128.8, 122.7, 117.9, 45.3, 37.5.

6.4.3 4-(2-Oxoimidazolidin-1-yl)benzene-1-sulfonyl chloride (51). To 1.5 mL (23.1 mmol) of chlorosulfonic acid in 3 mL of carbon tetrachloride at 0 °C was added slowly (3.1 mmol) compound **50**. The reaction was almost completed after 2 h at 0 °C. The reaction mixture was poured slowly onto ice water, filtered to collect the solid. The white solid was dried under vacuum. Yield: 56%; mp: 257-259 °C; IR v: 3232, 1711 cm⁻¹; ¹H NMR (DMSO-d₆): δ 7.57-7.51 (m, 4H, Ar), 3.88-3.82 (m, 2H, CH₂), 3.44-3.38 (m, 2H, CH₂); ¹³C NMR (DMSO-d₆): δ 158.9, 141.2, 140.5, 126.1, 115.8, 44.5, 36.5.

6.5 CoMSIA and CoMFA studies

All calculations were performed on SGI Onyx3800 supercomputer system and Windows system. SYBYL molecular modeling software package was used to perform the QSAR analysis [58]. In CoMSIA studies, an Sp³ carbon atom with a unit positive charge was used as a probe to evaluate five interaction fields: steric, electrostatic, hydrophobic, hydrogen bond donor, and hydrogen bond acceptor. All aligned molecules were set in a Cartesian coordinates box. The probe was used to calculate the field potentials in the box with a 2 Å grid resolution. In order to get an optimal QSAR models, different other descriptors were used to optimize the QSAR equation. Those descriptors involved in optimizing the QSAR analysis are molecular weight (MW), molecular volume (V), molar refractivity (MR), polar volume (PV), polar surface area (PSA), energy, and the similarity data of each compound to the hypothesis. In CoMFA studies, Tripos standard fields were used as CoMFA field classes and an Sp³ carbon atom with a unit positive charge was used as the probe to evaluate steric and electrostatic potentials at every lattice point. The resolution of the grid was 2 Å. Distance method was used to control the form of the Coulombic electrostatic energy calculation. A 30 Kcal/mol cutoff was used for steric and electrostatic field values. In addition to the CoMFA fields, all descriptors used in optimizing the CoMSIA models were also used in optimizing CoMFA

models. The thirty seven compounds used in the CoMSIA study were also used in CoMFA study as well. Initially all PIB-SA derivatives were selected to generate the CoMSIA model. Biological activities for this set of compounds is small, falling within the range of 10^{-6} to 10^{-7} M, and this led to challenges to obtain a perfect model of high R^2 value for LOO prediction. Different ways to generate the alignment were tried including: the generation of hypothesis model by using two of the most actives compounds (**20** and **27**), four of the most actives compounds (**20**, **22**, **27**, and **40**), and six of the most actives compounds (**15**, **20**, **22**, **27**, **40**, and **48**, Fig. 2A). The hypothesis generated from the alignment on six active compounds is pursued further for the generation of the CoMSIA model. The best R^2 values of LOO (leave-one-out) generated from it were 0.446 for IC_{50} in HT-29 cell line, 0.552 for IC_{50} in M21 cell line, and 0.465 for IC_{50} in MCF-7 cell line. From the predicting result, we removed four outliers (absolute predict value greater than 1.0): compound **18**, **27**, **35** and **46**, and the models were rebuilt.

Acknowledgment

This work was supported by the Canadian Institutes of Health Research (R.C.-G; Grant #MOP-79334 and #MOP-89707). S. Fortin is recipient of a studentship from the Canadian Institutes of Health Research (CGD-83623). We also acknowledge the technical expertise of Dr. Michel Déry for HPLC-MS experiments.

Supplementary material

Supplementary data related to this article can be found online at <http://www.sciencedirect.com>.

References

- [1] American Cancer Society. *Cancer Facts & Figures 2010*. Atlanta: American Cancer Society; 2010
- [2] International Agency for Research on Cancer, *World Cancer Report 2008*. World Health Organization
- [3] Organisation mondiale de la Santé et Union Internationale Contre le Cancer. 2005, *Action mondiale contre le cancer*. URL : <http://www.who.int/>. [accession april 26th, 2011].
- [4] J.K. Buolamwini, Novel anticancer drug discovery, *Curr. Opin. Chem. Biol.* 3 (1999) 500-509.
- [5] M.A. Jordan, L. Wilson, Microtubules as a target for anticancer drugs, *Nat. Rev. Cancer* 4 (2004) 253-265.
- [6] P.M. Checchi, J.H. Nettles, J. Zhou, J.P. Snyder, H.C. Joshi, Microtubule-interacting drugs for cancer treatment, *Trends Pharmacol. Sci.* 24 (2003) 361-365.
- [7] G. Attard, A. Greystoke, S. Kaye, J. De Bono, Update on tubulin-binding agents, *Pathol. Biol. (Paris)* 54 (2006) 72-84.
- [8] G.K. Chen, G.E. Duran, A. Mangili, L. Beketic-Oreskovic, B.I. Sikic, MDR 1 activation is the predominant resistance mechanism selected by vinblastine in MES-SA cells, *Brit. J Cancer* 83 (2000) 892-898.
- [9] C. Dumontet, G.E. Duran, K.A. Steger, L. Beketic-Oreskovic, B.I. Sikic, Resistance mechanisms in human sarcoma mutants derived by single-step exposure to paclitaxel (Taxol), *Cancer Res.* 56 (1996) 1091-1097.
- [10] D.M. Patterson, G.J. Rustin, Vascular damaging agents, *Clin. Oncol. (R. Coll. Radiol.)* 19 (2007) 443-456.
- [11] C. Kanthou, G.M. Tozer, Microtubule depolymerizing vascular disrupting agents: novel therapeutic agents for oncology and other pathologies, *Int. J. Exp. Pathol.* 90 (2009) 284-294.
- [12] N.H. Nam, Combretastatin A-4 analogues as antimetabolic antitumor agents, *Curr. Med. Chem.* 10 (2003) 1697-1722.
- [13] J.M. Dziba, R. Marcinek, G. Venkataraman, J.A. Robinson, K.B. Ain, Combretastatin A4 phosphate has primary antineoplastic activity against human anaplastic thyroid carcinoma cell lines and xenograft tumors, *Thyroid.* 12 (2002) 1063-1070.
- [14] H.L. Anderson, J.T. Yap, M.P. Miller, A. Robbins, T. Jones, P.M. Price, Assessment of pharmacodynamic vascular response in a phase I trial of combretastatin A4 phosphate, *J. Clin. Oncol.* 21 (2003) 2823-2830.

- [15] D. Simoni, R. Romagnoli, R. Baruchello, R. Rondanin, M. Rizzi, M.G. Pavani, D. Alloatti, G. Giannini, M. Marcellini, T. Riccioni, M. Castorina, M.B. Guglielmi, F. Bucci, P. Carminati, C. Pisano, Novel combretastatin analogues endowed with antitumor activity, *J. Med. Chem.* 49 (2006) 3143-3152.
- [16] J.P. Stevenson, M. Rosen, W. Sun, M. Gallagher, D.G. Haller, D. Vaughn, B. Giantonio, R. Zimmer, W.P. Petros, M. Stratford, D. Chaplin, S.L. Young, M. Schnall, P.J. O'Dwyer, Phase I trial of the antivasular agent combretastatin A4 phosphate on a 5-day schedule to patients with cancer: magnetic resonance imaging evidence for altered tumor blood flow, *J. Clin. Oncol.* 21 (2003) 4428-4438.
- [17] S. Aprile, E. Del Grosso, G.C. Tron, G. Grosa, In vitro metabolism study of combretastatin A-4 in rat and human liver microsomes, *Drug Metab. Dispos.* 35 (2007) 2252-2261.
- [18] S.L. Young, D.J. Chaplin, Combretastatin A4 phosphate: background and current clinical status, *Expert Opin. Inv. Drug* 13 (2004) 1171-1182.
- [19] S. Fortin, L. Wei, E. Moreau, J. Lacroix, M.-F. Côté, É. Petitclerc, L. P. Kotra, R. C.-Gaudreault, Design, synthesis, biological evaluation and structure-activity relationships of substituted phenyl 4-(2-oxoimidazolidin-1-yl)benzenesulfonates as new tubulin inhibitors mimicking combretastatin A-4, *J. Med. Chem. Manuscript ID: jm-2011-00488a* (submitted April 21th, 2011).
- [20] G.C. Tron, T. Pirali, G. Sorba, F. Pagliai, S. Busacca, A.A. Genazzani, Medicinal chemistry of combretastatin A4: present and future directions, *J. Med. Chem.* 49 (2006) 3033-3044.
- [21] C.T. Supuran, A. Casini, A. Scozzafava, Protease inhibitors of the sulfonamide type: anticancer, antiinflammatory, and antiviral agents, *Med. Res. Rev.* 23 (2003) 535-558.
- [22] A. Casini, A. Scozzafava, C.T. Supuran, Sulfonamide derivatives with protease inhibitory action as anticancer, antiinflammatory and antiviral agents, *Exp. Opin. Ther. Pat.* 12 (2002) 1307-1327.
- [23] K.M. Neff, J.J. Nawarskas, Hydrochlorothiazide versus chlorthalidone in the management of hypertension, *Cardiol. Rev.* 18 (2010) 51-56.
- [24] M.H. Parker, V.L. Smith-Swintosky, D.F. McComsey, Y. Huang, D. Brenneman, B. Klein, E. Malatynska, H.S. White, M.E. Milewski, M. Herb, M.F. Finley, Y. Liu, M.L. Lubin, N. Qin, R. Iannucci, L. Leclercq, F. Cuyckens, A.B. Reitz, B.E. Maryanoff, Novel, broad-spectrum anticonvulsants containing a sulfamide group: advancement of N-((benzo[b]thien-3-yl)methyl)sulfamide (JNJ-26990990) into human clinical studies, *J. Med. Chem.* 52 (2009) 7528-7536.
- [25] B.E. Maryanoff, S.O. Nortey, J.F. Gardocki, R.P. Shank, S.P. Dodgson, Anticonvulsant O-alkyl sulfamates. 2,3:4,5-Bis-O-(1-methylethylidene)-beta-D-fructopyranose sulfamate and related compounds, *J. Med. Chem.* 30 (1987) 880-887.
- [26] C.T. Supuran, A. Scozzafava, A. Casini, Carbonic anhydrase inhibitors, *Med. Res. Rev.* 23 (2003) 146-189.

- [27] C.T. Supuran, A. Casini, A. Mastrolorenzo, A. Scozzafava, COX-2 selective inhibitors, carbonic anhydrase inhibition and anticancer properties of sulfonamides belonging to this class of pharmacological agents, *Mini-Rev. Med. Chem.* 4 (2004) 625-632.
- [28] A.E. Boyd, 3rd, Sulfonylurea receptors, ion channels, and fruit flies, *Diabetes* 37 (1988) 847-850.
- [29] B. Shan, J.C. Medina, E. Santha, W.P. Frankmoelle, T.C. Chou, R.M. Learned, M.R. Narbut, D. Stott, P. Wu, J.C. Jaen, T. Rosen, P.B. Timmermans, H. Beckmann, Selective, covalent modification of β -tubulin residue Cys-239 by T138067, an antitumor agent with in vivo efficacy against multidrug-resistant tumors, *Proc. Natl. Acad. Sci. USA* 96 (1999) 5686-5691.
- [30] J.D. Berlin, A. Venook, E. Bergsland, M. Rothenberg, A.C. Lockhart, L. Rosen, Phase II trial of T138067, a novel microtubule inhibitor, in patients with metastatic, refractory colorectal carcinoma, *Clin. Colorectal Canc.* 7 (2008) 44-47.
- [31] S. Kirby, S.Z. Gertler, W. Mason, C. Watling, P. Forsyth, J. Aniagolu, R. Stagg, M. Wright, J. Powers, E.A. Eisenhauer, Phase 2 study of T138067-sodium in patients with malignant glioma: Trial of the National Cancer Institute of Canada Clinical Trials Group, *Neuro-Oncology* 7 (2005) 183-188.
- [32] K. Yoshimatsu, A. Yamaguchi, H. Yoshino, N. Koyanagi, K. Kitoh, Mechanism of action of E7010, an orally active sulfonamide antitumor agent: inhibition of mitosis by binding to the colchicine site of tubulin, *Cancer Res.* 57 (1997) 3208-3213.
- [33] A.M. Mauer, E.E. Cohen, P.C. Ma, M.F. Kozloff, L. Schwartzberg, A.I. Coates, J. Qian, A.E. Hagey, G.B. Gordon, A phase II study of ABT-751 in patients with advanced non-small cell lung cancer, *J. Thorac. Oncol.* 3 (2008) 631-636.
- [34] J. Michels, S.L. Ellard, L. Le, C. Kollmannsberger, N. Murray, E.S. Tomlinson Guns, R. Carr, K.N. Chi, A phase IB study of ABT-751 in combination with docetaxel in patients with advanced castration-resistant prostate cancer, *Ann. Oncol.* 21 (2010) 305-311.
- [35] K.W. Yee, A. Hagey, S. Verstovsek, J. Cortes, G. Garcia-Manero, S.M. O'Brien, S. Faderl, D. Thomas, W. Wierda, S. Kornblau, A. Ferrajoli, M. Albitar, E. McKeegan, D.R. Grimm, T. Mueller, R.R. Holley-Shanks, L. Sahelijo, G.B. Gordon, H.M. Kantarjian, F.J. Giles, Phase 1 study of ABT-751, a novel microtubule inhibitor, in patients with refractory hematologic malignancies, *Clin. Cancer Res.* 11 (2005) 6615-6624.
- [36] J.A. Segreti, J.S. Polakowski, K.A. Koch, K.C. Marsh, J.L. Bauch, S.H. Rosenberg, H.L. Sham, B.F. Cox, G.A. Reinhart, Tumor selective antivascular effects of the novel antimetabolic compound ABT-751: an in vivo rat regional hemodynamic study, *Cancer Chemother. Pharmacol.* 54 (2004) 273-281.
- [37] J.P. Liou, K.S. Hsu, C.C. Kuo, C.Y. Chang, J.Y. Chang, A novel oral indoline-sulfonamide agent, N-[1-(4-methoxybenzenesulfonyl)-2,3-dihydro-1H-indol-7-yl]-isonicotinamide (J30), exhibits potent activity against human cancer cells in vitro and

- in vivo through the disruption of microtubule, *J. Pharmacol. Exp. Ther.* **323** (2007) 398-405.
- [38] J.Y. Chang, H.P. Hsieh, C.Y. Chang, K.S. Hsu, Y.F. Chiang, C.M. Chen, C.C. Kuo, J.P. Liou, 7-Aroyl-aminoindoline-1-sulfonamides as a novel class of potent antitubulin agents, *J. Med. Chem.* **49** (2006) 6656-6659.
- [39] C.G. Wermuth. *The practice of medicinal chemistry*. 3rd ed. Amsterdam ; Boston: Elsevier/Academic Press 2008.
- [40] J. Neville, A.; J. Lim, J.; Su, D.-S.;R. Wood, M. MERCK & CO., INC. Arylsulfonamide derivatives. Patent. International Application No. PCT/US2004/021018.
- [41] E.R. Parmee, E.M. Naylor, L. Perkins, V.J. Colandrea, H.O. Ok, M.R. Candelore, M.A. Cascieri, L. Deng, W.P. Feeney, M.J. Forrest, G.J. Hom, D.E. MacIntyre, R.R. Miller, R.A. Stearns, C.D. Strader, L. Tota, M.J. Wyvratt, M.H. Fisher, A.E. Weber, Human β 3 adrenergic receptor agonists containing cyclic ureidobenzenesulfonamides, *Bioorg. Med. Chem. Lett.* **9** (1999) 749-754.
- [42] National Cancer Institute (NCI/NIH), Developmental therapeutics program human tumor cell line screen, URL : <http://dtp.nci.nih.gov/branches/btb/ivclsp.html>, [accession February 2nd, 2011].
- [43] M.J. Schibler, F. Cabral, Taxol-dependent mutants of Chinese hamster ovary cells with alterations in α - and β -tubulin, *J. Cell Biol.* **102** (1986) 1522-1531.
- [44] F. Cabral, M.E. Sobel, M.M. Gottesman, CHO mutants resistant to colchicine, colcemid or griseofulvin have an altered β -tubulin, *Cell* **20** (1980) 29-36.
- [45] W.T. Beck, T.J. Mueller, L.R. Tanzer, Altered surface membrane glycoproteins in Vinca alkaloid-resistant human leukemic lymphoblasts, *Cancer Res.* **39** (1979) 2070-2076.
- [46] X.F. Hu, T.J. Martin, D.R. Bell, M. de Luise, J.R. Zalcborg, Combined use of cyclosporin A and verapamil in modulating multidrug resistance in human leukemia cell lines, *Cancer Res.* **50** (1990) 2953-2957.
- [47] S. Fortin, J. Lacroix, M.-F. Côté, E. Moreau, E. Petitclerc, R. C.-Gaudreault, Quick and simple detection technique to assess the binding of antimicrotubule agents to the colchicine-binding site, *BPO [Online]* **12** (2010) 113-117, DOI: 10.1007/s12575-010-9029-5
- [48] A.N. Jain, Morphological similarity: a 3D molecular similarity method correlated with protein-ligand recognition, *J. Comput.-Aided Mol. Des.* **14** (2000) 199-213.
- [49] S. Struski, P. Cornillet-Lefebvre, M. Doco-Fenzy, J. Dufer, E. Ulrich, L. Masson, N. Michel, N. Gruson, G. Potron, Cytogenetic characterization of chromosomal rearrangement in a human vinblastine-resistant CEM cell line: use of comparative genomic hybridization and fluorescence in situ hybridization, *Cancer Genet. Cytogenet.* **132** (2002) 51-54.

- [50] K. Ueda, C. Cardarelli, M.M. Gottesman, I. Pastan, Expression of a full-length cDNA for the human "MDR1" gene confers resistance to colchicine, doxorubicin, and vinblastine, *Proc. Natl. Acad. Sci. USA* 84 (1987) 3004-3008.
- [51] E. Petitclerc, R.G. Deschesnes, M.F. Cote, C. Marquis, R. Janvier, J. Lacroix, E. Miot-Noirault, J. Legault, E. Mounetou, J.C. Madelmont, R. C.-Gaudreault, Antiangiogenic and antitumoral activity of phenyl-3-(2-chloroethyl)ureas: a class of soft alkylating agents disrupting microtubules that are unaffected by cell adhesion-mediated drug resistance, *Cancer Res.* 64 (2004) 4654-4663.
- [52] E. Petitclerc, A. Boutaud, A. Prestayko, J. Xu, Y. Sado, Y. Ninomiya, M.P. Sarras, Jr., B.G. Hudson, P.C. Brooks, New functions for non-collagenous domains of human collagen type IV. Novel integrin ligands inhibiting angiogenesis and tumor growth in vivo, *J. Biol. Chem.* 275 (2000) 8051-8061.
- [53] J. Kim, W. Yu, K. Kovalski, L. Ossowski, Requirement for specific proteases in cancer cell intravasation as revealed by a novel semiquantitative PCR-based assay, *Cell* 94 (1998) 353-362.
- [54] T. Uchibayashi, S.W. Lee, K. Kunimi, M. Ohkawa, Y. Endo, M. Noguchi, T. Sasaki, Studies of effects of anticancer agents in combination with/without hyperthermia on metastasized human bladder cancer cells in chick embryos using the polymerase chain reaction technique, *Cancer Chemother. Pharmacol.* 35 Suppl (1994) S84-87.
- [55] P.C. Brooks, S. Silletti, T.L. von Schalscha, M. Friedlander, D.A. Cheresh, Disruption of angiogenesis by PEX, a noncatalytic metalloproteinase fragment with integrin binding activity, *Cell* 92 (1998) 391-400.
- [56] U.K. Laemmli, Cleavage of structural proteins during the assembly of the head of bacteriophage T4, *Nature* 227 (1970) 680-685.
- [57] M.A. Lyu, Y.K. Choi, B.N. Park, B.J. Kim, I.K. Park, B.H. Hyun, Y.H. Kook, Overexpression of urokinase receptor in human epidermoid-carcinoma cell line (HEp3) increases tumorigenicity on chorio-allantoic membrane and in severe-combined-immunodeficient mice, *Int. J. Cancer* 77 (1998) 257-263.
- [58] SYBYL, 8.1, Tripos International, 1699 South Hanley Rd., St. Louis, Missouri, 63144, USA.